Osipyan Institute of Solid State Physics of Russian Academy of Sciences

as a manuscript

Bobkova Irina Vyacheslavovna

SPIN PHENOMENA IN SUPERCONDUCTING HETEROSTRUCTURES

Dissertation Summary
for the purpose of obtaining academic degree Doctor of Science in Physics
in the speciality 1.3.3 "Theoretical physics"

Chernogolovka
2023

The dissertation was prepared at Osipyan Institute of Solid State Physics of Russian Academy of Sciences

Dissertation topic

Relevance. In recent decades, a new field of physics, spintronics, has been developing. It includes a wide range of fundamental phenomena associated with the presence of a spin degree of freedom in many-body systems, as well as a large number of both already implemented and under development proposals for using the spin for storing, transmitting and using information. Spintronics is a rapidly developing, multidisciplinary field. A number of modern textbooks and many reviews are devoted to its individual aspects. In modern society, there is an urgent need for the development of energy-saving technologies. Therefore, a special place in the field of spintronics is occupied by low-dissipation spintronics, which at the moment is mainly represented by two large areas - magnonics of magnetic insulators and superconducting spintronics [1, 2]. This dissertation is devoted to the theoretical study of a certain range of issues of superconducting spintronics.

The specifics of the effects introduced into spintronics by superconducting elements can be conventionally divided into several groups. The first group of effects is associated with the non-dissipativity of spin-polarized currents carried by triplet Cooper pairs [1, 2]. Standard spintronic effects such as spin-transfer torque, spin-orbit torque and the magnetization switching or motion of magnetic defects caused by these torques can be generated by non-dissipative spin currents in structures with triplet superconductivity, for example, S/F heterostructures or triplet superconductors, as well as superconductors with spin-orbit interaction.

The second group of effects is determined by the remarkable properties of weak superconductivity in Josephson junctions, which are currently the basic elements of quantum electronics. For example, using a ferromagnet as a weak link, one can obtain the phase difference π in the ground state of a Josephson junction [3]. Such π-junctions are widely used as elements of superconducting quantum systems. In addition, it is possible to realize a phase difference φ_0 intermediate between zero and π in the ground state of the Josephson junction. Such junctions can serve as phase batteries. For a long time, the search for physical principles and technological solutions has been carried out to create a superconducting transistor based on a Josephson junction with controlled switching between the superconducting and normal states. It is expected that such systems can serve as the element base of an energy-saving superconducting computer, as well as in the field of quantum information.

The third group of effects is associated with the presence of a superconducting gap in the density of states of a superconductor, which leads to a strong energy dependence of the density of states near the Fermi level. In Zeeman-split superconductors, this dependence acquires particle-hole asymmetry in each spin subband separately, while the total particle-hole symmetry of two spin subbands is conserved in total. This remarkable property of a superconductor leads to the presence of giant thermoelectric and thermospin effects [4] in superconductors and forms the basis of superconducting spin caloritronics, providing almost the highest possible efficiency of heat-to-spin conversion.

Magnetoelectric effects in superconducting structures should be singled out as a separate group. Generally speaking, the essence of magnetoelectric effects is the appearance of a connection between the electric current and the spin degrees of freedom in the system. Magnetoelectric effects in non-superconducting systems are well known. The reason for the occurrence of magnetoelectric effects is the presence of a spin-orbit interaction in the system or the inhomogeneity of the magnetization, which in the local spin basis can also be reduced to an effective spin-orbit interaction. The presence of superconducting elements in the system brings fundamentally new physics into magnetoelectric effects. First, the generation of spin polarization by supercurrent becomes a non-dissipative process. Secondly, it turns out that

the inverse magnetoelectric effect often manifests itself not by the generation of an electric current in response to the application of a Zeeman field, but by the appearance of an exotic phase-inhomogeneous, so-called helical state of the superconductor. In Josephson junctions, the inverse magnetoelectric effect is realized as an anomalous phase shift in the ground state [5,6]. Recently, there has been an understanding that the inverse magnetoelectric effect in superconductor/magnet heterostructures is an extremely important physical phenomenon, since provides a direct connection between the magnetization of the magnet and the phase of the superconducting condensate, which is a macroscopic quantum quantity.

The next group includes the principles of the interaction of magnetic moments through the superconducting state. The indirect exchange interaction between magnetic moments carried by conduction electrons in a metal (RKKY-interaction) is well known. This interaction provides antiferromagnetic coupling between magnetic layers in GMR structures and spin valves. However, the strongly oscillating and damping character of this interaction on atomic scales makes it possible to achieve interaction between magnetic moments at characteristic distances not exceeding several nanometers in individual layered structures. In recent years, research has been actively carried out in which the nonmagnetic interlayer between magnets in spin valves is replaced by a superconductor. The characteristic scale of the interaction of magnets through a superconductor is the superconducting coherence length, at which the proximity effect with the magnet manifests itself in the superconductor, or the penetration depth of the magnetic field, if the interaction is based on the electromagnetic proximity effect [7]. The inverse magnetoelectric effect in superconducting heterostructures, providing a connection between the magnetic moment and the superconducting phase, makes it possible to implement a fundamentally different way of using the features of the superconducting state to establish a long-range indirect interaction between magnetic moments, proposed in the dissertation [8].

In addition, the study of the influence of spin effects on the superconducting state itself is of great fundamental and applied importance. It is well known that superconductivity and ferromagnetism are two antagonistic types of ordering. While in traditional singlet superconductors Cooper pairs consist of electrons with opposite spins, ferromagnetic order implies the same direction of electron spins. Therefore, in particular, equilibrium uniform singlet superconductivity cannot coexist with magnetism above the so-called paramagnetic limit of superconductivity when the exchange energy h exceeds $\Delta/\sqrt{2}$, where Δ is the value of the superconducting order parameter at zero exchange field. However, a number of very interesting effects are predicted in the coexistence region. In particular, the emergence of a spatially inhomogeneous superconducting Larkin-Ovchinnikov-Fulde-Ferrell (LOFF) [9, 10] state, spatial oscillations of the condensate wave function in a ferromagnet (a mesoscopic analog of the LOFF state), as well as partial conversion of singlet correlations into triplet ones, which strongly interact with each other [11, 12]. The described proximity effects are already being used in applied superconducting electronics. Of particular interest, both from the fundamental point of view and from the point of view of spintronic applications and applications of superconducting electronics, is the issue of external control of superconductivity, including triplet superconductivity. Controlled $0-\pi$ transitions are of great interest.

The goal of this work is to study the fundamental features of spin phenomena in superconductors and to search for effects that are of potential interest for applied superconducting spintronics.

To achieve this goal, it was necessary to solve the following **tasks**:

1. To study the effect of various types of nonequilibrium distribution of quasiparticles on the superconducting state, including the weak superconductivity of Josephson junc-

tions, in the presence of a Zeeman field in a superconductor.

2. To develop a theory of the thermospin effect in superconductors with Zeeman splitting of the density of states. On its basis, to explain the experimental data on the observation of a weakly decaying spin imbalance in nonlocal experimenters on superconducting films in a parallel magnetic field or superconductor/ferromagnet heterostructures. To study the effect of temperature-induced spin imbalance on the superconducting state in Zeeman-split superconductors. To develop a theory of thermally induced motion of magnetic defects in superconductor/magnet hybrids based on the giant thermospin effect. To estimate the expected efficiency of thermally induced motion of defects in comparison with known experimental data on non-superconducting structures.

3. To study the manifestations of the inverse magnetoelectric effect, specific for the superconducting state - the helical state and the anomalous shift of the phase difference in the ground state of Josephson junctions - in systems with inhomogeneous magnetization.

4. To investigate the fundamental mechanism of long-range interaction of magnetic moments via the condensate phase, based on the inverse magnetoelectric effect.

5. To study the features of magnetoelectric effects in superconducting heterostructures with 3D topological insulators.

6. To develop a generalization of the quasiclassical theory that successively includes the terms necessary to describe the direct magnetoelectric effect in superconducting heterostructures with spin-orbit interaction.

7. To study one more superconducting magnetoelectric effect - generation of triplet correlations by moving condensate. To derive effective equations to describe the effect. In particular, to study the dynamic generation of triplet correlations by a high-frequency electric field. To explore the potential use for the creation of high-frequency superconducting transistors and photo-magnetic devices.

With all the variety of problems considered in the dissertation, they are all devoted to the study of the fundamental features of the superconducting state in the presence of a Zeeman field of various physical nature, the study of exotic types of pair correlations induced under such conditions and their influence on the magnetic subsystem.

Key results

Research methods. To solve the set problems, which include the description of superconductivity, magnetism and dynamic effects, a combination of the quasiclassical theory of superconductivity in terms of Green's functions and the Landau-Lifshitz-Gilbert equation to describe magnetic dynamics is used. Most of the tasks posed are related to the description of nonequilibrium effects, so the Keldysh technique is used to calculate the Green's functions. Problems related to magnetoelectric effects require a generalization of the standard quasiclassical theory to the case of taking into account the exchange field or spin-orbit interaction beyond the limits of the quasiclassical approximation. The corresponding generalizations of the theory are developed in the dissertation.

Main results submitted for defense:

1. The superconducting state in thin films in the presence of a Zeeman field under nonequilibrium conditions has been studied. The dependences of the superconducting order parameter on the magnitude of the control parameter (voltage) and temperature are calculated when a nonequilibrium spin imbalance is created in a superconductor. It is shown that when a certain spin imbalance is created in the system, the superconductivity suppressed by the Zeeman field is partially recovered and can exist above the paramagnetic limit of superconductivity.

2. The effect of various nonequilibrium modes on the Josephson current in superconductor/ferromagnet/superconductor junctions has been studied. It is shown that the creation of a symmetric charge-neutral energy disequilibrium or spin imbalance can sharply increase the decay length of triplet correlations in a ferromagnet in a controlled way. In turn, this leads to a sharp increase in the Josephson current through the junction. The creation of a spin imbalance makes it possible to obtain a controlled $0-\pi$ transition with a sufficiently strong exchange field of the ferromagnet compared to T_c. In the case of a weak exchange field of order T_c, to obtain controlled $0-\pi$ transitions, it is sufficient to create an energy (spin-neutral and charge-neutral) nonequilibrium. The transition between the 0 and π states occurs due to the controlled population of different regions of the sign-alternating current-carrying density of states.

3. A theory of a long-range spin imbalance in a Zeeman split superconductor has been developed. The theoretical results are in good qualitative agreement with the experimental data.

4. The effect of thermally induced spin imbalance on the superconducting state in a Zeeman field has been studied. The effects of thermally induced suppression and enhancement of superconductivity have been predicted.

5. A theory of thermally induced motion of magnetic domain walls in thin-film bilayer superconductor/ferromagnet and superconductor/antiferromagnet structures has been developed. It is predicted that the efficiency of this mechanism based on the giant thermospin effect, i.e. the speed of motion that can be achieved for a given temperature difference, should greatly exceed its value for thermally induced motion, reported in experiments for non-superconducting structures.

6. A generalization of the quasiclassical theory has been obtained, which successively takes into account first-order corrections in the ratio of the spin-orbit splitting to the Fermi energy. Based on this theory, triplet correlations in some superconducting heterostructures with spin-orbit interaction and the direct magnetoelectric effect in ballistic Josephson junctions through a metal with spin-orbit interaction have been calculated.

7. A generalization of quasiclassical equations has been developed for describing superconducting heterostructures with a topological insulator for the nonequilibrium case and for describing superconductivity induced at the surface conducting layer of a topological insulator by the proximity effect with a conventional superconductor.

8. For heterostructures with topological insulators, a giant magnetoelectric effect in the density of states and, as a consequence, the effect of supercurrent-controlled spin filtering has been predicted.

9. The effect of splitting of the easy axis of a ferromagnet in Josephson junctions with a composite weak link, which is a ferromagnet/topogical insulator bilayer, has been predicted.

10. A long-range mechanism of pairwise interaction of magnetic moments through the condensate phase based on the inverse magnetoelectric effect has been predicted. A specific implementation of this interaction in a system of coupled Josephson junctions has been studied.

11. The effect of generation of long-range triplet correlations by a moving condensate has been predicted. Effective boundary conditions were derived for the Usadel equations, which allow one to calculate the effect. The corresponding triplet correlations were calculated in systems where the condensate motion is realized by Meissner currents screening an external magnetic field, as well as by the application of an alternating electric field. The Josephson current was calculated through a junction in which long-range triplets are generated by a condensate. Possible experiments to observe the effect were proposed. It was proposed to use the effect to create superconducting transistors, photo-magnetic devices and controlled $0 - \pi$ junctions.

12. A theory of the direct and inverse magnetoelectric effect in thin-film superconductor/inhomogeneous ferromagnet hybrids has been developed. Generalized quasiclassical equations were formulated taking into account the terms responsible for magnetoelectric effects. Based on the developed theory, the helical state in bilayers with a helical ferromagnet and the state with a spontaneous phase difference in bilayers with a domain wall were studied. The torques caused by the supercurrent flowing through the superconducting part on the magnetization were calculated. An analytical calculation is applicable for the case when the characteristic size of the magnetic inhomogeneity exceeds the superconducting coherence length.

13. A theory of the direct and inverse magnetoelectric effect in Josephson junctions through a strong ferromagnet has been developed. It was shown that the Josephson current is capable of inducing the dynamics of the magnetization of a ferromagnet in the weak link region, but in this case the junction passes into a special resistive state even at currents less than the critical one. This state is characterized by the presence of voltage at the junction, but the absence of normal current through it and, accordingly, the Joule losses in it. And the work done by the current source goes to compensate for the Gilbert damping in the magnetic subsystem. This voltage is induced by magnetic dynamics through the inverse magnetoelectric effect and can be used for electrical detection of magnetization dynamics.

14. It has been shown that supercurrent induces a new type of chiral interaction between magnetic moments. It is triple. The symmetry of the interaction energy with respect to time reversal is ensured by the fact that the interaction constant is an odd function of the supercurrent. Specific implementations of the effect in a system of magnetic impurities placed in a superconducting matrix and in a Josephson junction through non-coplanar magnetic structures were studied.

Author's personal contribution to the results submitted for defense consists in setting tasks, carrying out analytical calculations, discussing the results obtained, and preparing manuscripts for publications.

Scientific novelty. All results submitted for defense are new. In the case of items 2, 6, 7, they partially generalize the results obtained earlier by other authors - then a comparison with previous results discussed in the text and references are given. In the cases of items 3, 12 and 13, there are results independently and simultaneously obtained by other authors, which partially intersect with the results submitted for defense. Relevant discussion and references to the literature are also included in the text. Such a comparison simultaneously confirms the reliability of the presented results.

Practical significance. Developed in the thesis methods and results can be used to describe a wide range of phenomena in superconducting spintronics. Via proposed approaches and based on the results obtained, it is possible further development of the theory of spin caloritronics and magnetoelectric effects in superconducting heterostructures. All the results obtained can be applied to the analysis of experimental data. In some cases, such data are already available, and comparison shows good agreement between theory and experiment. Many predicted effects, such as, for example, triplet correlations induced by condensate motion, thermally induced motion of domain walls, and the dynamics of magnetic moments in a system of coupled Josephson junctions, can serve as a motivation for new experiments. A number of the results obtained have the potential for application in the field of low-dissipation spintronics.

Reliability of the obtained results is ensured by the reliability of the applied theoretical methods, agreement with the theoretical results obtained in other works, and agreement with the data of experiments performed by other authors.

Publications and approbation of research.

The numbering of publications in the lists of publications of the advanced level and the standard level corresponds to the numbering of the list of publications of the author in the dissertation text.

Publications of the advanced level:

[P1] I.V. Bobkova and A.M. Bobkov, Recovering the superconducting state via spin accumulation above the pair breaking magnetic field of superconducting/ferromagnet multilayers, Phys. Rev. B **84**, 140508(R) (2011).

[P3] T. E. Golikova, M. J. Wolf, D Beckmann, G. A. Penzyakov, I. E. Batov, I. V. Bobkova, A. M. Bobkov and V. V. Ryazanov, Controllable supercurrent in mesoscopic superconductor-normal metal-ferromagnet crosslike Josephson structures, Supercond. Sci. Technol. **34**, 095001 (2021).

[P4] I.V. Bobkova and A.M. Bobkov, Triplet contribution to the Josephson current in the nonequilibrium superconductor/ferromagnet/superconductor junction, Phys. Rev. B **82**, 024515 (2010).

[P5] I.V. Bobkova and A.M. Bobkov, Long-range proximity effect for opposite-spin pairs in superconductor-ferromagnet heterostructures under nonequilibrium quasiparticle distribution, Phys. Rev. Lett. **108**, 197002 (2012).

[P7] I. V. Bobkova, A. M. Bobkov, Injection of nonequilibrium quasiparticles into Zeeman-split superconductors: A way to create long-range spin imbalance, Phys. Rev. B **93**, 024513 (2016).

[P8] I. V. Bobkova and A. M. Bobkov, Thermospin effects in superconducting heterostructure, Phys. Rev. B **96**, 104515 (2017).

[P9] I. V. Bobkova, A. M. Bobkov, and Wolfgang Belzig, Thermally induced spin-transfer torques in superconductor/ferromagnet bilayers, Phys. Rev. B **103**, L020503 (2021).

[P10] G. A. Bobkov, I. V. Bobkova, A. M. Bobkov, and Akashdeep Kamra, Thermally induced spin torque and domain-wall motion in superconductor/antiferromagnetic-insulator bilayers, Phys. Rev. B **103**, 094506 (2021).

[P11] I. V. Bobkova, A. M. Bobkov, Quasiclassical theory of magnetoelectric effects in superconducting heterostructures in the presence of spin-orbit coupling, Phys. Rev. B **95**, 184518 (2017).

[P12] I. V. Bobkova, A. M. Bobkov, Alexander A. Zyuzin, and Mohammad Alidoust, Magnetoelectrics in disordered topological insulator Josephson junction", Phys. Rev. B **94**, 134506 (2016).

[P13] I. V. Bobkova and A. M. Bobkov, Electrically controllable spin filtering based on superconducting helical states, Phys. Rev. B **96**, 224505 (2017).

[P14] M. Nashaat, I. V. Bobkova, A. M. Bobkov, Yu. M. Shukrinov, I. R. Rahmonov, and K. Sengupta, Electrical control of magnetization in superconductor/ferromagnet/superconductor junctions on a three-dimensional topological insulator, Phys. Rev. B **100**, 054506 (2019).

[P15] G. A. Bobkov, I. V. Bobkova, and A. M. Bobkov, Long-range interaction of magnetic moments in a coupled system of superconductor-ferromagnet-superconductor Josephson junctions with anomalous ground-state phase shift, Phys. Rev. B **105**, 024513 (2022).

[P16] M. A. Silaev, I. V. Bobkova, and A. M. Bobkov, Odd triplet superconductivity induced by a moving condensate, Phys. Rev. B **102**, 100507(R) (2020).

[P17] I.V. Bobkova, A.M. Bobkov, and M.A. Silaev, Dynamic Spin-Triplet Order Induced by Alternating Electric Fields in Superconductor-Ferromagnet-Superconductor Josephson Junctions, Phys. Rev. Lett. **127**, 147701 (2021).

[P18] A. A. Mazanik and I. V. Bobkova, Supercurrent-induced long-range triplet correlations and controllable Josephson effect in superconductor/ferromagnet hybrids with extrinsic spin-orbit coupling, Phys. Rev. B **105**, 144502 (2022).

[P19] I.V. Bobkova, A.M. Bobkov, and M.A. Silaev Gauge theory of the long-range proximity effect and spontaneous currents in superconducting heterostructures with strong ferromagnet, Phys. Rev. B **96**, 094506 (2017).

[P20] I. V. Bobkova, A. M. Bobkov, and M. A. Silaev, Spin torques and magnetic texture dynamics driven by the supercurrent in superconductor/ferromagnet structure, Phys. Rev. B **98**, 014521 (2018).

[P21] D.S. Rabinovich, I. V. Bobkova, A. M. Bobkov, and M. A. Silaev, Chirality selective spin interactions mediated by the moving superconducting condensate, Phys. Rev. B **98**, 184511 (2018).

[P22] D.S. Rabinovich, I.V. Bobkova, A.M. Bobkov, and M.A. Silaev, Resistive State of Superconductor-Ferromagnet-Superconductor Josephson Junctions in the Presence of Moving Domain Wall, Phys. Rev. Lett. **123**, 207001 (2019).

[P23] D. S. Rabinovich, I. V. Bobkova, A. M. Bobkov, and M. A. Silaev, Magnetoelectric effects in superconductor/ferromagnet bilayers, Phys. Rev. B **99**, 214501 (2019).

[P24] I. V. Bobkova, A. M. Bobkov, and M. A. Silaev, Magnetoelectric effects in Josephson junctions (Topical Review), J. Phys.: Condens. Matter **34** 353001 (2022).

Publications of the standard level:

[P2] I. V. Bobkova, A. M. Bobkov, Recovering of superconductivity in S/F bilayers under spin-dependent nonequilibrium quasiparticle distribution, Pis'ma v ZhETF, **101**, 442 (2015) [JETP Lett. **101**, 407 (2015)].

[P6] I. V. Bobkova, A. M. Bobkov, Long-range spin imbalance in mesoscopic superconductors under Zeeman splitting, Pis'ma v ZhETF, **101**, 124 (2015) [JETP Lett. **101**, 118 (2015)].

Talks at conferences and seminars. The main results of the dissertation were reported at international conferences: "Nanophysics and nanoelectronics" (Nizhnii Novgorod, 2010, 2012, 2014, 2015, 2016, 2018, 2020, 2021, 2022), International conference on superconductivity and magnetism (Turkey, 2014, 2018, 2021), International workshop on superconducting spintronics "SUPERSPIN15" (Norway, 2015) , International conference "Interaction of Superconductivity and Magnetism in Nanosystems" (Moscow, 2015), MIPT conference and International School "Superconducting hybrid nanostructures: physics and applications" (Dolgoprudny, 2016), WE-Heraeus-Seminar "Trends in mesoscopic superconductivity" (Germany, 2016), Moscow International Symposium on Magnetism (Moscow, 2017), XIII-th Rencontres du Vietnam, Nanophysics: from Fundamentals to Applications (Vietnam, 2017), International Scientific meeting "Non-equilibrium superconductivity and spintronics" (UK, 2019), Workshop "Superconductivity in low-dimensional and interacting systems" (Germany, 2019), VII Euro-Asian Symposium "Trends in MAGnetism" (Ekaterinburg, 2019), Coherent order and transport in spin-active systems: Interplay between magnetism and superconductivity, SPICE online workshop (Germany, 2020, online), All-Russian Scientific and Practical Conference "Nature. Man. Society", (Dubna, 2021, online), International Conference on Low-dimensional materials: theory, modeling, experiment (LDM2021, Dubna, 2021), Trends in MAGnetism 2021 (Italy, 2021, online), 2021 Molecular Foundry User Meeting (USA, 2021, online).

Also, the results of the dissertation were reported and discussed at seminars at the Institute of Solid State Physics RAS (Chernogolovka), MIPT (Dolgoprudny), at the Kurchatov Institute (Moscow), at JINR (Dubna), at the IPM RAS (Nizhny Novgorod), at the University of Konstanz (Germany), at the Center for Quantum Spintronics (QuSpin, Norway).

Contents

Introduction substantiates the relevance of the topic, formulates the goal of the work, the novelty and practical value of the results obtained are substantiated, the content of the dissertation by chapters is described.

The first chapter is devoted to the study of the superconducting state in the presence of the Zeeman field under nonequilibrium conditions. All results presented in this section were obtained in collaboration with A.M. Bobkov and published in papers **[P1,P2]** from the author's list of publications on the topic of the dissertation. As an introduction, a short review of the formalism of quasiclassical Keldyshev Green's functions is given, in the technique of which calculations are carried out. A classification of possible independent types of nonequilibrium distribution is also carried out.

Section **1.1** investigates the effect of spin imbalance on superconducting thin-film ferromagnet/superconductor structures, in which, under equilibrium conditions, superconductivity is partially or completely suppressed as a result of proximity to the ferromagnet. It is well known that the interaction of conduction electrons with an exchange or magnetic field

(now only the Zeeman effect of a magnetic field is considered) destroys superconductivity. If the exchange energy h in the Hamiltonian of the conduction electrons of a superconductor exceeds the value $h = \Delta/\sqrt{2}$ (the paramagnetic limit of superconductivity [13]), then the homogeneous superconducting state becomes energetically unfavorable. An inhomogeneous (LOFF) superconducting state has also been predicted for such systems [9, 10], but can only exist in a narrow range of exchange fields above the paramagnetic limit. A thin-film superconductor in contact with a ferromagnet behaves similarly to a superconductor in an exchange field; therefore, superconductivity in it is also destroyed by a sufficiently strong ferromagnet. This subsection shows that the creation of a spin-dependent disequilibrium in such a superconductor can partially restore superconductivity and, under certain conditions, maintain its existence above the paramagnetic limit.

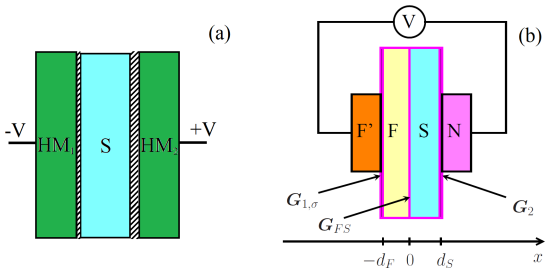

Figure 1: Sketches of structures in which the effect of nonequilibrium recovering of superconductivity is considered. (a) A thin film superconductor sandwiched between two half-metals; (b) thin film superconductor/weakly ferromagnetic alloy bilayer. Additional ferromagnetic (F') and normal (N) electrodes are needed to create a spin imbalance in the bilayer.

The effect of nonequilibrium recovery of superconductivity is considered in two hybrid structures. The first structure is a thin-film superconductor with a thickness less than or of the order of the coherence length ($d \lesssim \xi_S$) located between two half-metals, see Fig. 1(a). The second structure is a thin film superconductor/weakly ferromagnetic alloy bilayer, Fig. 1(b). In such structures, due to the proximity to the ferromagnet superconductivity is suppressed by two factors: the effective exchange field h_{eff} and the depairing factor Γ, which is physically responsible for the leakage of pairs into the ferromagnet and their subsequent destruction there. Voltage is applied to both structures as shown in Fig. 1(a)-(b). Then, as shown in **[P1]**, in the structure shown in Fig. 1(a), neglecting spin relaxation processes in the superconductor, the nonequilibrium distribution function takes the form $\varphi_{\uparrow,\downarrow} = \tanh[(\varepsilon \pm eV)/2T]$. That is, a spin imbalance $2eV$ appears in the system, as shown in the inset to Fig. 2(a). The behavior of the superconducting order parameter in the system shown in Fig. 1(a) with such a distribution function is shown in Fig. 2(a)-(b). Fig. 2(a) demonstrates the dependence of the order parameter at zero temperature on the applied voltage for different values of the effective exchange field. It can be seen that at $V = 0$ superconductivity does not exist for high fields exceeding the paramagnetic limit. But as the voltage increases, superconductivity arises and the order parameter reaches its maximum value at $eV = h_{eff}$. The mathematical

reason for this can be easily seen from the self-consistency equation for the order parameter:

$$\frac{1}{\lambda} = \int_{-\omega_D}^{\omega_D} \frac{d\varepsilon}{4} \left\{ \mathrm{Re}\left[\frac{\mathrm{sgn}(\varepsilon + h_{eff})}{\sqrt{(\varepsilon + i\Gamma + h_{eff})^2 - \Delta^2}} \right] \tanh \frac{\varepsilon + eV}{2T} \right.$$
$$\left. + \mathrm{Re}\left[\frac{\mathrm{sgn}(\varepsilon - h_{eff})}{\sqrt{(\varepsilon + i\Gamma - h_{eff})^2 - \Delta^2}} \right] \tanh \frac{\varepsilon - eV}{2T} \right\}. \quad (1)$$

By changing the integration variable, it is easy to show that the effect of the spin imbalance on the wave function of the condensate is equivalent to the effect of the effective exchange field, and under the condition $eV = h_{eff}$ their effect is mutually compensated. A more physical explanation of the effect is that the creation of such an electronic distribution of quasiparticles, as shown in the inset to Fig.2(a), creates optimal conditions for the pairing of electrons with opposite momenta, compensating for the destructive effect of the exchange field. The corresponding mechanism is discussed in detail in the text of the dissertation. It is also seen from Fig.2(a) that in the absence of h_{eff}, the spin imbalance also suppresses superconductivity, which once again illustrates the equivalence of their action. Fig. 2(b) shows the dependence of the order parameter on temperature. The gray curve corresponds simply to the bulk value of the order parameter. The black one shows the suppression due to Γ at $h_{eff} = 0$ and equilibrium distribution of electrons. The dotted curve illustrates that when h_{eff} is above the paramagnetic limit (when superconductivity is not realized under equilibrium conditions) and the optimal choice of spin imbalance, superconductivity is restored to values at $h_{eff} = 0$. Thus, the depairing effect of the exchange field can be completely compensated by the spin imbalance. The dotted curve illustrates that when the spin imbalance optimality condition is violated, superconductivity is suppressed, as in the case of a nonzero but lower value of h_{eff}.

It is known that under equilibrium conditions the transition to the normal state at $h_{eff} = \Delta/\sqrt{2}$ occurs by the first order. Here, such a transition, which corresponds to the depairing of all pairs and the appearance of a nonzero difference in the number of normal electrons with spins up and down, is impossible, because electronic distribution is fixed by external conditions.

Figures 2(c)-(d) demonstrate the influence of spin flip processes on the effect of nonequilibrium recovery of superconductivity. Spin flip processes smear the distribution function in the superconductor and thus prevent the complete recovery. But for realistic parameters, the recovery effect exists, including above the paramagnetic limit.

Work **[P2]** investigates the same effect for a slightly different system shown in Fig. 1(b). The advantage of this model is that it corresponds to the already experimentally realized superconductor/weakly ferromagnetic alloy bilayers. The suppression of the critical temperature by an effective exchange field in such a system under equilibrium conditions has been well studied both theoretically and experimentally. The dependences of the critical temperature on the thickness of the ferromagnetic layer calculated by us are shown in Fig. 3(a). When voltage is applied to the system, a spin dependence of the distribution function also arises in it. A typical view of the resulting distribution function is shown in Fig. 3(b). A certain disadvantage of this system compared to the previous one is the weaker spin dependence of the distribution function, which is associated with the absence of half-metallic elements. Nevertheless, in **[P2]** it is shown that the effect of superconductivity recovering can be observed in this case as well. The dependence of the critical temperature of the system on the applied voltage is shown in Fig.3(c).

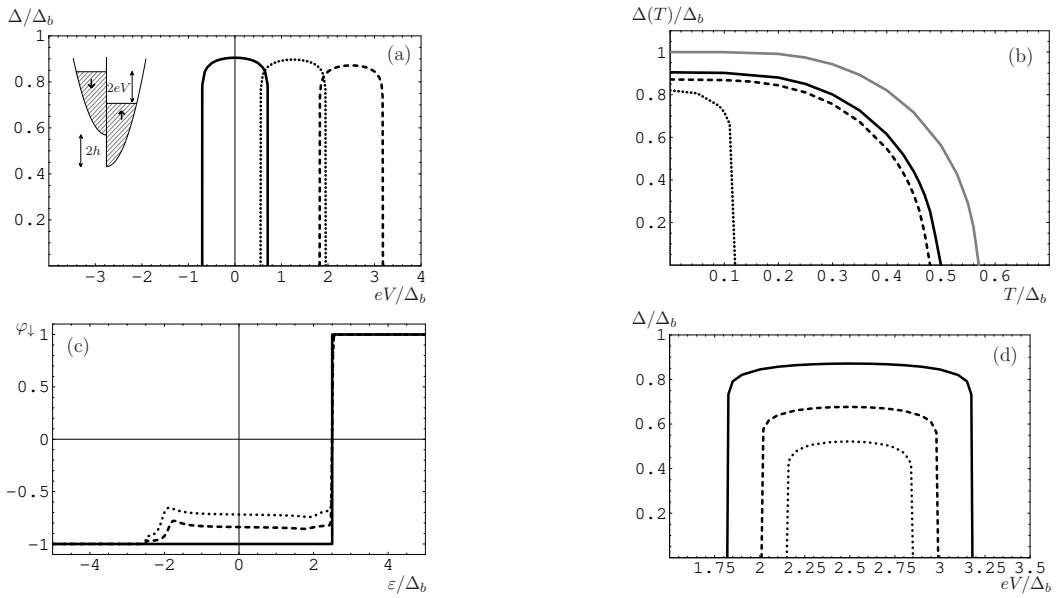

Figure 2: (a) Dependence of $\Delta(T=0)$ on eV. $h_{eff}=0$ (solid); $h_{eff}=1.25$ (dotted) $h_{eff}=2.5$ (dashed). All energy quantities are measured in units of the order parameter in the bulk of the superconductor. Insert: population of spin subbands $\uparrow, \downarrow$ for the considered nonequilibrium distribution. (b) Temperature dependence of Δ. The gray line is $\Delta(T)$ in a bulk superconductor, the black solid line is $\Delta(T, h_{eff}=eV=0)$, the dashed line is $\Delta(T, h_{eff}=eV=2.5)$, dotted - $\Delta(T, h_{eff}=2.5, eV=3.1)$.(c) Distribution function $\varphi_{\downarrow}(\varepsilon)$ for different values of the inverse spin relaxation time. (d) Dependence of $\Delta(eV)$ for $h_{eff}=2.5$ and different values of the inverse spin relaxation time.

Section **1.2** investigates the effect of various nonequilibrium modes on the Josephson current in superconductor/ferromagnet/superconductor (S/F/S) junctions. Subsection **1.2.1** investigates the effect of charge-neutral disequilibrium on the Josephson current through an S/F/S junction. A typical distribution function is shown in Fig. 5(a). Such a distribution function is created by passing a normal current (injection current) through the weak link region of a cross-like Josephson S/(N/F)/S structure, see Fig. 4(a)-(b). The created distribution is a two-step function antisymmetric in energy in each of the spin subbands. In this case, both the total charge and the total spin of the quasiparticles accumulated in the weak link region are equal to zero. The nonequilibrium is the sum of the energy mode $f_L=(\varphi_\uparrow+\varphi_\uparrow)/2$ and the spin-energy mode $f_{L3}=(\varphi_\uparrow-\varphi_\uparrow)/2$ [4]. The critical current of the junction can be represented as the product of the so-called current-carrying density of states (SCDOS) and the distribution function integrated over all energies:

$$j_c=\frac{d}{4eR_{NF}}\int_{-\infty}^{\infty}d\varepsilon f_L(\varepsilon)J_\varepsilon, \tag{2}$$

where J_ε is SCDOS. In the case under consideration, only the spin-independent energy mode f_L contributes to the current. SCDOS is a sign-changing function of energy. Positive and negative regions contribute to the current with opposite signs. By changing the nonequilibrium population of different energy levels, it is possible to achieve a change in the sign of the critical current, i.e. the transition of the junction from 0 to π-state. It is known that this physical mechanism makes it possible to implement an injection-controlled 0-π transition in an S/N/S junction [14]. In subsection **1.2.1** it is shown that the presence of a ferromagnet in the weak link region makes it possible to obtain a double 0-π junction controlled by injection.

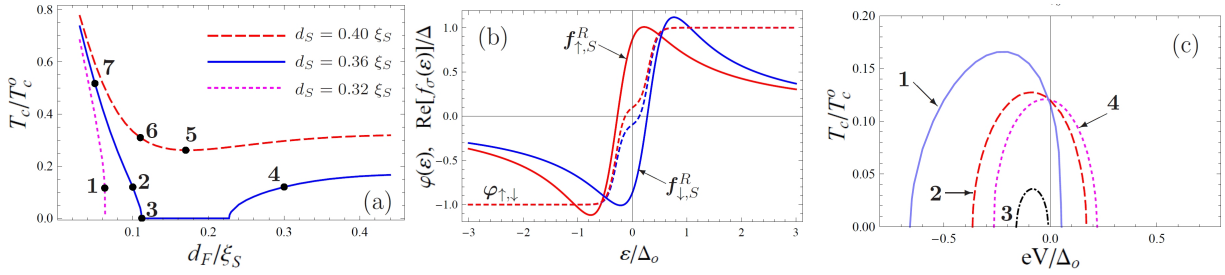

Figure 3: (a) S/F bilayer critical temperature as a function of F-layer thickness for different S-layer thicknesses. (b) Characteristic behavior of the distribution function (dashed line) and the anomalous Green's function (solid line) as functions of the quasiparticle energy. (c) Critical temperature of the bilayer as a function of applied voltage. The parameters of the curves correspond to the numbers that are marked on the panel (a).

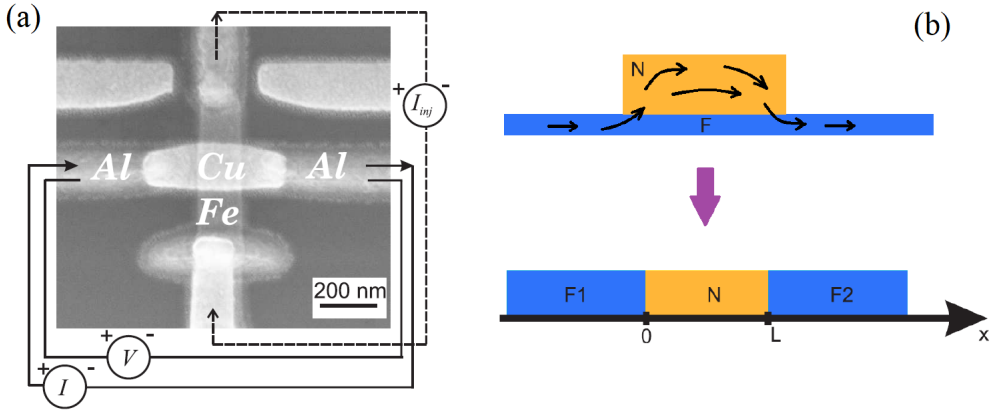

Figure 4: (a) SEM image of a cross-like S/(N/F)/S structure, top view. (b) Schematic representation of the weak link region, which is a normal metal (Cu) lying on a ferromagnet (Fe), side view. The trajectories of the injection current flow are shown. Also shown is an effective one-dimensional structure model that was used to calculate the distribution function.

This is due to the fact that, owing to the presence of an effective exchange field in the weak link region, SCDOS in S/(N/F)/S has 2 sign change points at $\varepsilon > 0$, in contrast to a normal weak link, where such a point only one. The number of such points determines the number of possible 0-π-transitions. The SCDOS for the considered S/(N/F)/S junction and the critical current as a function of the injection current, showing 2 0-π transitions, are shown in Fig. 5. These theoretical results are in qualitative agreement with the experimental results. The theoretical results of this subsection were obtained in collaboration with A.M. Bobkov and published in **[P3]** from the list of the author's publications on the topic of the dissertation, which also presents experimental results obtained by a group of our experimental colleagues T. Golikova, M. Wolf, D. Beckman, G. Penzyakov, I Batov and V. Ryazanov.

In subsection **1.2.2**, the effect of spin imbalance on the Josephson current through the S/F/S junction is studied. Actually SCDOS in S/F/S contact depends on the spin. Therefore, we can introduce such concepts as the singlet and triplet parts of SCDOS $J_{\varepsilon,s(t)} = (J_{\varepsilon,\uparrow} \pm J_{\varepsilon,\downarrow})/2$. The energy-antisymmetric distribution function considered in the previous subsection interacts only with the singlet part of SCDOS. At sufficiently high val-

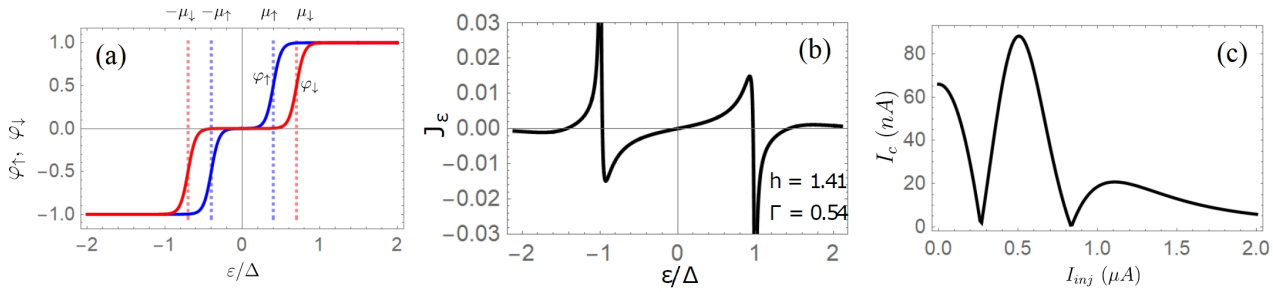

Figure 5: (a) A typical view of the distribution function, which is created by passing the injection current in the weak link of the Josephson junction shown in Fig. 4. (b) SCDOS as a function of quasiparticle energy. The values of the effective Zeeman field and the effective depairing parameter for which this dependence is constructed are shown in the figure in units of the superconducting gap in the leads. (c) Critical current of the Josephson junction as a function of injection current.

ues of the exchange field in the ferromagnetic weak link $h \gg \Delta$, which just corresponds to the experimental parameters of S/F/S junctions through ferromagnetic alloys (not complex F/N interlayers, as considered in the previous subsection), the singlet part of SCDOS is concentrated in the region $\varepsilon \approx \Delta$ and loses its sign changing behavior, see Fig. 6(a). This closes the possibility of implementing controlled 0-π-transitions based on the antisymmetric distribution function. In this subsection, we show that the creation of a nonequilibrium distribution containing a spin imbalance mode makes it possible to obtain controlled 0-π transitions in this case as well. The physics of the effect is that the spin imbalance in the Josephson current interacts with the triplet part of the SCDOS and the corresponding contribution to the current is an antisymmetric function of the spin imbalance. This makes it possible to control the sign of the total critical current using the magnitude and sign of the spin imbalance. In the limit of tunnel S/F interfaces, the critical current has the form:

$$j_c \propto |\Delta| e^{-d/\xi_F} \left[\sqrt{2}\pi \cos\left(\frac{d}{\xi_F} + \frac{\pi}{4}\right) + \frac{1}{\sqrt{2}} \log \left| \frac{|\Delta| + eV_{b\uparrow}}{|\Delta| - eV_{b\uparrow}} \right| \sin\left(\frac{d}{\xi_F} + \frac{\pi}{4}\right) \right] , \qquad (3)$$

where $eV_{b\uparrow}$ is the value of the spin imbalance. The first term in square brackets is the contribution of the singlet part of SCDOS and, in the considered approximations, does not depend on the degree of nonequilibrium of the system, and the second term is the contribution of the triplet part of SCDOS, which is controlled by the spin imbalance. The typical behavior of the singlet and triplet parts of SCDOS is shown in Fig. 6(a)-(b), and the 0-π transition controlled by the spin imbalance is shown in Fig. 6(c). The results of this subsection were obtained in collaboration with A.M. Bobkov and published in **[P4]** from the author's list of publications on the topic of the dissertation.

It is well known that, under equilibrium conditions at $h \gg \Delta$, pairs with opposite spins penetrate into the weak link region of the S/F/S junction to a distance of the order of the magnetic coherence length $\xi_F = \sqrt{D/h}$, which small and usually of the order of a few nanometers. Only pairs with equal spins penetrate to much larger distances of the order of the normal coherence length $\xi_N = \sqrt{D/2\pi T_c}$. Subsection **1.2.3** discusses a special type of nonequilibrium distribution that makes it possible to sharply increase the depth of penetration of pairs with opposite spins into a Josephson junction, thereby sharply increasing the amplitude of the critical Josephson current.

An example of a system in which it is possible to create a suitable non-equilibrium

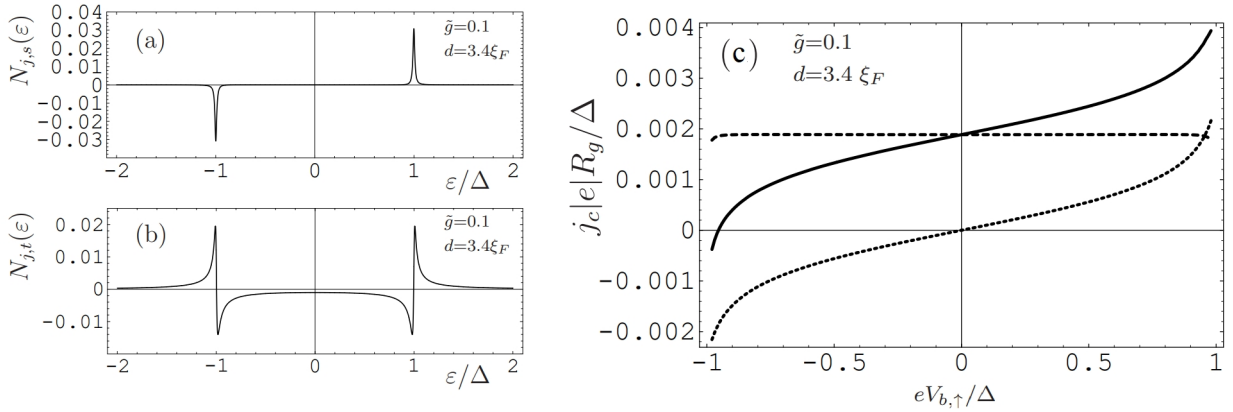

Figure 6: Singlet (a) and triplet (b) SCDOS components for Josephson S/F/S junction with $h \gg \Delta$. (c) Critical Josephson current as a function of the magnitude of the spin imbalance. The contributions of the SCDOS singlet component (dashed line) and the triplet component (dotted) are shown separately. The solid curve represents the total critical current.

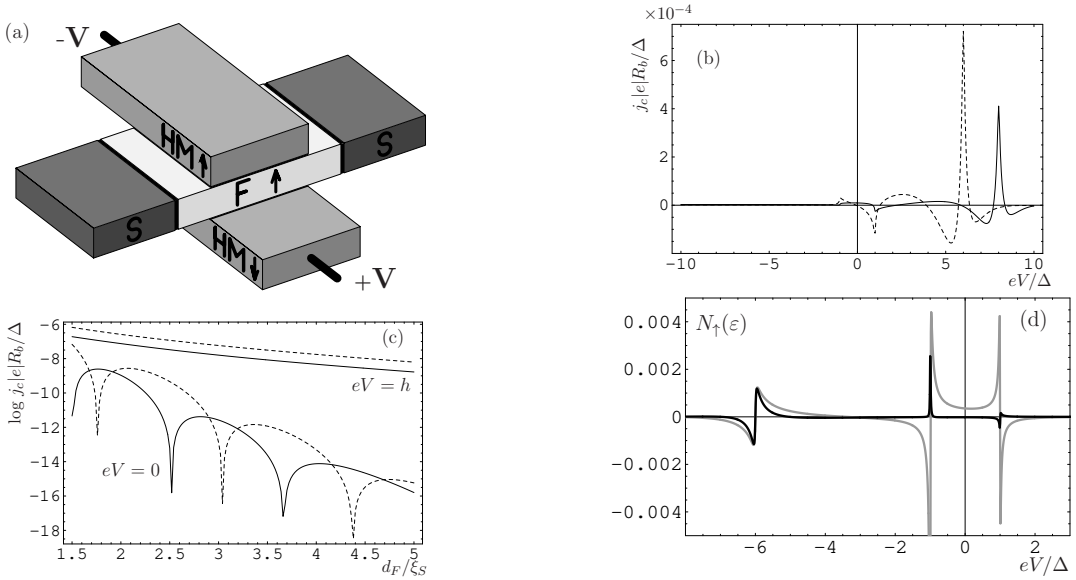

Figure 7: (a) Sketch of the system considered in subsection **1.2.3**. (b) Critical Josephson current as a function of eV. $h = 8\Delta$ (solid line), 6Δ (dotted line). $d_F = 3\xi_S$. (c) Critical current as a function of d_F. $h = 8\Delta$ (solid line), 6Δ (dashed line). (d) SCDOS $N_\uparrow$ for the spin-up subband as a function of ε for $h = 6\Delta$ and $d_F = 2.5\xi_S$ (black line), $1.5\xi_S$ (gray line). $N_\downarrow(\varepsilon) = -N_\uparrow(-\varepsilon)$. $T = 0.01\Delta$ for all graphs.

distribution is shown in Fig. 7(a). Additional half-metallic electrodes are attached to the weak link region of the Josephson S/F/S junction, between which a voltage is applied. As a result, a nonequilibrium distribution of the form $\varphi_{\uparrow,\downarrow} = \tanh[(\varepsilon \pm eV)/2T]$ is created in the weak link region, which is a combination of the energy mode and the spin imbalance mode. The value of the created spin imbalance is $2eV$. Fig. 7(b) shows the dependencies of the critical Josephson current as a function of the applied voltage. The critical current has a sharp peak at $eV = h$. This is due to a sharp increase in the decay length of pairs with opposite spins in the ferromagnet. The physical explanation of the effect is as follows. The exchange field leads to the appearance of a nonzero momentum of the Cooper pair in a

ferromagnet and, as a consequence, fast oscillations of the wave function of the Cooper pairs, the phase of which depends on the direction. In a diffusive ferromagnet, such correlations are effectively suppressed as a result of path averaging. The creation of different population levels for up and down spins (spin imbalance) compensates for the nonzero momentum of the Cooper pair. For $eV = h$ the compensation is complete. The decay length is equal to the normal coherence length, which greatly increases the overlap of condensate wave functions penetrating from opposite S/F interfaces and, as a result, the amplitude of the critical current. It is also seen in Fig. 7(b) that the critical current is an alternating function of the voltage, i.e. voltage-controlled 0-π-transitions appear in the system. For $eV \ll h$ this effect was studied in the previous subsection.

The dependence of the critical current on the length of the ferromagnetic weak link is shown in Fig. 7(c). This figure clearly demonstrates that under equilibrium conditions at $eV = 0$ the critical current decays on the scale ξ_F simultaneously oscillating with a period of $2\pi\xi_F$, while the critical current at $eV = h$ decays at ξ_N and does not exhibit oscillations, which is a characteristic feature of long-range correlations with zero total momentum of the pair. The results of this subsection were obtained in collaboration with A.M. Bobkov and published in **[P5]** from the author's list of publications on the topic of the dissertation.

The Second chapter is devoted to the study of some effects of spin caloritronics in S/F structures. It turns out that the Zeeman-split superconducting state, which is formed in such heterostructures, realizes practically the maximum possible efficiency of heat-to-spin conversion. This makes superconductor/magnet structures extremely interesting and promising objects for spin caloritronics. The basic physical effect that ensures the conversion of heat into spin is the so-called giant spin-dependent Seebeck effect or giant thermospin effect [4]. The physics of this effect is considered as an introduction to the second chapter. Next, some physical manifestations, consequences of this effect, and possibilities of application in spintronics are considered.

In section **2.1**, a theory is developed that describes the generation of a nonequilibrium spin signal in superconductors with Zeeman splitting from a spinless (thermal) nonequilibrium. Spin imbalance in a normal metal or superconductor is often measured in non-local experiments. The detector is a ferromagnetic electrode, and the current measured at this electrode has the form $I_D = G_D(\mu + P_D S)$, where G_D is the conductance of the superconductor/detector interface, μ is the shift of the quasiparticle chemical potential determined by the charge imbalance in superconductor, P_D is the polarization of the detector, and S is the magnitude of the spin imbalance. Thus, the difference in nonlocal signals for two opposite polarization directions of the detector gives the magnitude of the spin imbalance in the superconductor. It was found experimentally [15–18] that in Zeeman-split superconductors, the spin imbalance relaxation length is of the order of several microns, which greatly exceeds its values in normal metals and superconductors without Zeeman splitting $\sim 400 - 500$ nm.

The dissertation shows that in Zeeman-split superconductors the spin signal measured by the detector has the form:

$$S = -\frac{1}{2}\int d\varepsilon \Big[N_s f_{T3} + N_t (f_L - \tanh\frac{\varepsilon}{2T}) \Big], \tag{4}$$

where $N_{s,t} = (N_\uparrow \pm N_\downarrow)$ is the total density of states and the difference in the densities of states with spin up and down, respectively. In superconductors with the Zeeman splitting $N_t \neq 0$, therefore, the contribution to the spin accumulation S is made not only by the difference in the distribution functions for spins up and down, expressed by the nonequilibrium mode f_{T3}, but also by the spinless nonequilibrium energy mode f_L. In the dissertation, all densities

of states and distribution functions in the system under consideration are calculated within the framework of the nonequilibrium quasiclassical Green's functions approach. It is shown that f_{T3} and f_L have completely different relaxation mechanisms and decay lengths in a superconductor. While the decay length of the spin imbalance f_{T3} is mainly determined by the elastic processes of spin relaxation on magnetic or spin-orbital impurities and is just hundreds of nanometers in order of magnitude, the energy mode f_L relaxes to its equilibrium value $\tanh[\varepsilon/2T]$ on the scales of inelastic electron-electron and electron-phonon relaxation. The former are of the order of several microns, while the latter, depending on the system, are of the order of several microns to several tens of microns. Electron-electron relaxation processes thermalize the distribution of injected quasiparticles, but do not change their total energy, and electron-phonon relaxation processes remove energy from the electronic subsystem, thus eliminating the overheating of the electronic subsystem.

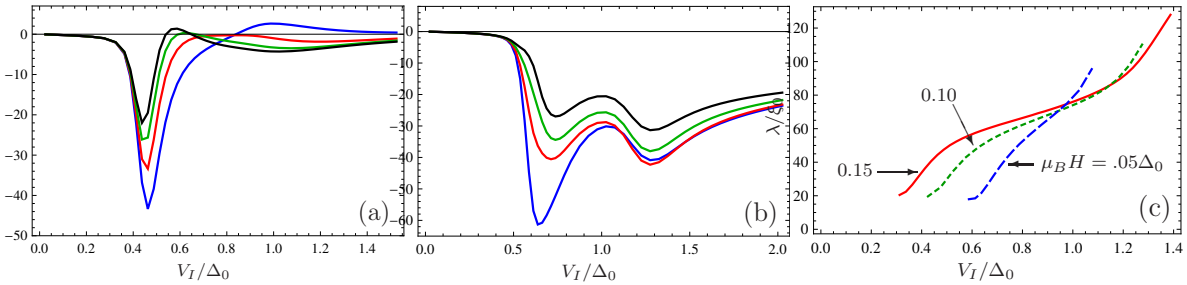

Figure 8: (a) and (b) Total conductance as a function of V_I at different distances from the injector: $L = 5, 15, 25, 35\xi_0$. For (a) the overheating of the electronic subsystem is small, $\mu_B H = 0.22\Delta_0$, $h_{int} = 0$. For (b) the overheating of the electronic subsystem is significant, $\mu_B H = 0.05\Delta_0$, $h_{int} \approx 0.22\Delta_0$. Other system parameters are given in the full text of the dissertation. (c) Total conductance relaxation length versus V_I. Different curves correspond to different applied magnetic fields. The parameters are the same as for panel (b).

Figs. 8(a)-(b) show the results of calculating the nonlocal conductance dS/dV_I, where V_I is the voltage in the injector circuit. Fig. 8(a) corresponds to the case of good thermal contact of the superconductor with the substrate, when there is practically no overheating in the electronic subsystem of the superconductor, and Fig. 8(b) demonstrates nonlocal conductance for the case of poor thermal contact when overheating occurs in the electronic subsystem. These results reproduce well all the main features of a nonlocal spin signal experimentally found in [15–18]: (i) dS/dV_I is an antisymmetric function of the injection voltage, which is completely inexplicable if the measured nonequilibrium spin is generated by the difference in the distribution functions of quasiparticles with spin up and down, i.e. f_{T3}. (ii) according to the experimental data [17] the signal decay length increases with the injection voltage. This is shown in Fig. 8(c). In the framework of the developed theory, this is due to the different scales of the electron-electron and electron-phonon interactions. As shown in the dissertation, the nonlocal spin conductance for high injection voltages is mainly associated with electron overheating, and, therefore, relaxes on the scales of the electron-phonon interaction.

The results of this section were obtained in collaboration with A.M. Bobkov and published in **[P6,P7]** from the author's list of publications on the topic of the dissertation.

Section **2.2** is devoted to studying the effect of thermally induced spin imbalance on the superconducting state in thin films of superconductors with Zeeman splitting. The sketches of the structures under consideration are shown in the insets to Figs. 9(a),(c). This is a superconductor/normal metal bilayer. A temperature difference is created between the layers.

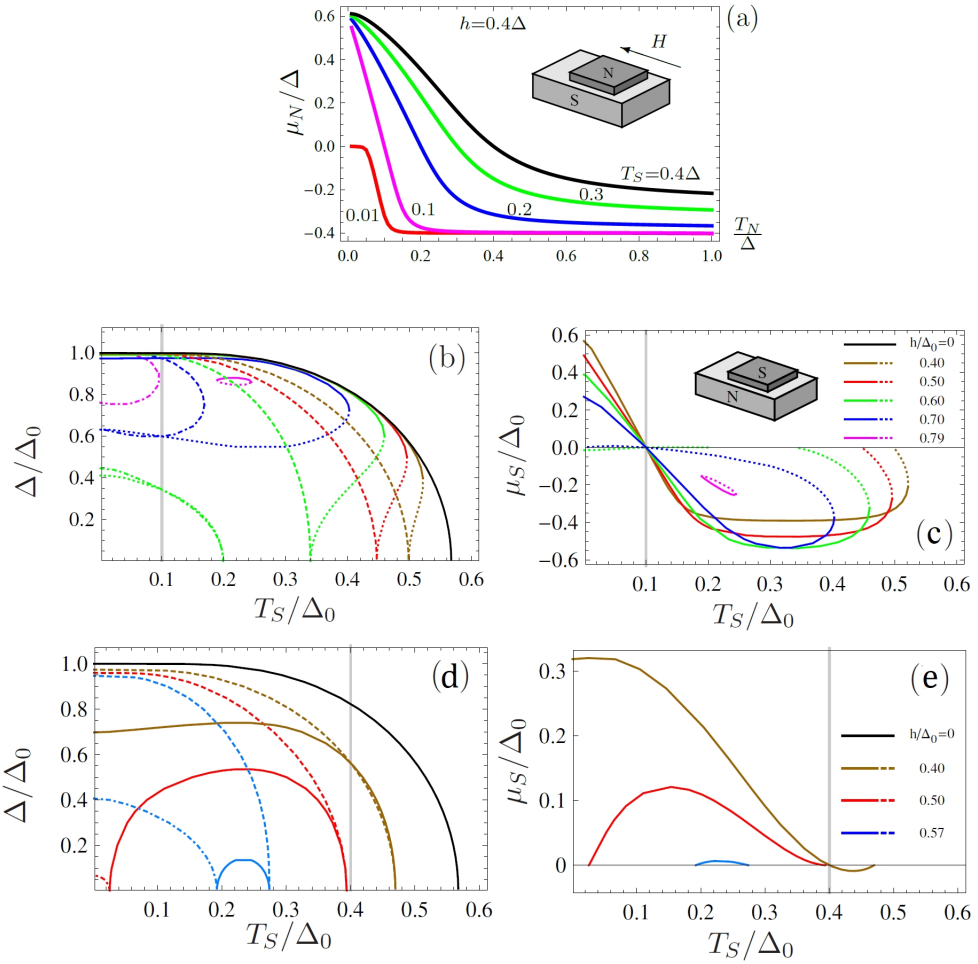

Figure 9: (a) Spin imbalance accumulated in a normal metal as a function of T_N. Different curves correspond to different temperatures T_S of the superconducting reservoir. (b) Superconducting order parameter for $T_N = 0.1\Delta_0$ (vertical gray line) as a function of T_S. Here $\Delta_0 \equiv \Delta(T_S = T_N = 0, h = 0)$. Different colors correspond to different applied magnetic fields. The dashed lines are the results of calculating the order parameter at $\mu_S = 0$ (the parts of the curves depicted by the dashed-dotted lines are absolutely unstable branches of the solutions corresponding to the free energy maximum). The solid lines are the results taking into account the correct value of the spin imbalance. (c) Corresponding spin imbalance μ_S as a function of T_S. (d) Superconducting order parameter for $T_N = 0.4\Delta_0$ as a function of T_S. (e) μ_S as a function of T_S for panel parameters (d).

One of the layers is large and is a spin reservoir, the distribution of electrons in it is always considered to be equilibrium, and the other layer has a limited size and a spin imbalance induced by the temperature difference can occur in it if a Zeeman splitting of the density of states is created in the superconductor, for example, by applying a parallel magnetic field to the system. The reason for this effect is the spin current that flows through the S/N boundary when a temperature difference is created on it and the Zeeman distribution is present in the superconductor. It is important to note that the efficiency of heat-to-spin conversion in such a system is close to the maximum possible, since almost all quasiparticles participating in the creation of the flow through the boundary carry spin in the same direction. This is referred to in the literature as the "giant spin-dependent Seebeck effect".

Let us first consider the case when a normal layer has limited dimensions. The spin imbalance in it is determined from the condition that the spin current through the boundary is equal to zero for a given temperature difference (the size of the N-layer is considered small compared to the spin relaxation length). The result of calculating the spin imbalance as a function of the N-layer temperature is shown in Fig. 9(a). Its characteristic features are: (i) for $T_N \ll T_S$ $\mu_N \to \Delta \mathrm{sgn} h - h$ and (ii) for $T_N \gg T_S$ $\mu_N \to -h$. These quantities determine the maximum value of thermally induced spin imbalance that can be created in the system under consideration. Taking into account the equilibrium spin accumulation $S = N_F h$ in a normal metal in the presence of an applied field, the total spin accumulation $S = N_F(h + \mu_N)$ tends to the value $S = N_F \Delta \mathrm{sgn} h$ in the limit $T_N \ll T_S$ and $S = 0$ in the inverse limit $T_N \gg T_S$. Thus, an interesting situation arises here, which can be qualitatively described as follows: in the limit $T_N \ll T_S$, a normal metal behaves like a ferromagnet with an approximately constant magnetic moment, and in the opposite case $T_N \gg T_S$ this behavior is similar to the behavior of a superconductor at zero temperature.

Let us now turn to the case when the superconductor has limited dimensions. This case is somewhat more complicated, since the value of the superconducting order parameter in a superconductor strongly depends on h, μ_S, and T_S and must be calculated self-consistently. The results of calculating the spin imbalance for this case, taking into account the self-consistency of the order parameter, are shown in Fig.9(c) and (e). The behavior of the spin imbalance depending on the temperature of the superconductor has, at first glance, a completely different character. But, in fact, the order parameter tends to the same limits as in the case of a normal metal, i.e. $\mu_S \to \Delta \mathrm{sgn} h - h$ for $T_S \ll T_N$ and $\mu_S \to -h$ for $T_S \gg T_N$. The difference in the curves for the case of imbalance in a normal metal and a superconductor is due to the suppression of the order parameter by the exchange field and temperature, since it is obvious that the giant thermospin effect takes place only in the superconducting state, and therefore $\mu_S \to 0$ at $\Delta \to 0$.

Let us now consider how thermally induced spin imbalance affects superconductivity in a confined superconductor. Let the temperature of a normal reservoir be low. The behavior of the order parameter as a function of the superconductor temperature is shown in Fig. 9(b). It can be seen that in this case the generation of a spin imbalance leads to the restoration of superconductivity suppressed by the Zeeman field. The order parameter tends to its value without the Zeeman field. The explanation for this behavior is that the spin imbalance tends to $\mu_S = -h$, i.e. the chemical potential in each of the spin subbands individually becomes exactly in the middle of the superconducting gap, and this position of the chemical potential ensures the minimum number of thermal quasiparticles that destroy superconductivity at a given temperature. In the opposite case of the high temperature of a normal reservoir, the spin imbalance effectively increases the Zeeman field in the superconductor. This increase is strongest at the lowest temperatures of the superconductor, which leads to a very unusual behavior of the order parameter with temperature, which is shown in Fig. 9(d). The order parameter increases with temperature, and at higher values of the Zeeman field, a superconducting phase can appear at finite temperatures from a nonsuperconducting low-temperature state. The results of this section were obtained in collaboration with A.M. Bobkov and published in **[P8]** from the author's list of publications on the topic of the dissertation.

Section **2.3** predicts the possibility of highly efficient thermally induced motion of domain walls in thin-film superconductor/ferromagnet and superconductor/antiferromagnet bilayers. Sketches of thin-film bilayer S/F and S/AF systems containing a domain wall are shown in Fig. 10(a) and (b). Opposite ends of the bilayers are maintained at different temperatures.

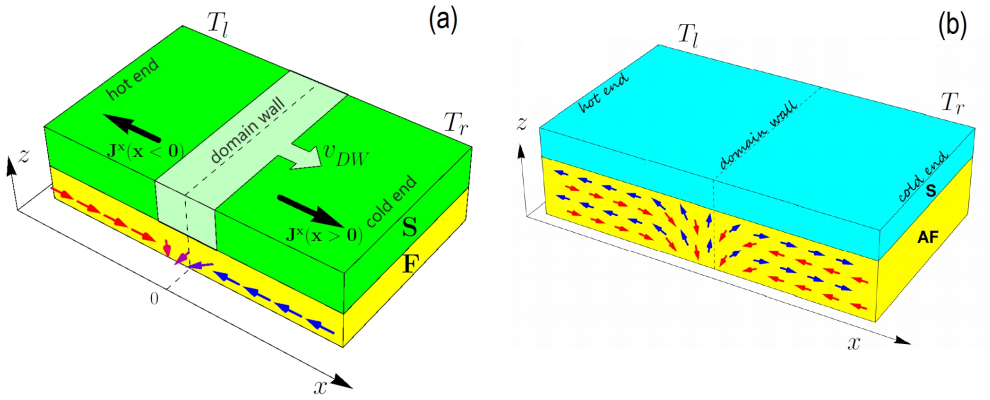

Figure 10: Sketches of S/F (a) and S/AF (b) bilayers. The magnetization of a ferromagnet F or an antiferromagnet AF has the form of a head-to-head domain wall (DW) and is shown by arrows. The figure in panel (a) illustrates the process of thermally induced pumping into the DW region. Panel (b) shows that there is uncompensated magnetization at the S/AF boundary. The blue arrows show the spin of the sublattice A, and the red arrows show the spin of the sublattice B. In both cases, the temperature difference $T_l - T_r$ is applied along the x direction.

This causes the domain wall to move from the hot end to the cold end. The motion of the domain wall is caused by the giant thermospin effect. Qualitatively, the effect is explained as follows. The ferromagnet induces an effective exchange field in the superconductor, which leads to the Zeeman splitting of the density of states in it. The induced exchange field is parallel to the magnetization of the ferromagnet. Therefore, in a superconductor, it also forms a domain wall and has opposite directions in different domains. Then, in each "domain" of the superconductor, we have a Zeeman-split superconductor, at the ends of which a temperature difference is created. This leads to the appearance of a purely spin current in it by the mechanism of the giant thermospin effect. Since in both domains the effective exchange field has different signs, and the temperature gradient has the same direction, these spin currents flow in opposite directions, thus pumping a spin of a certain sign into the region of the domain wall. The conservation of angular momentum forces the wall to move. If a nonzero surface magnetization occurs at the AF/S interface of the bilayer with the antiferromagnet (and this case is considered in the dissertation), then the mechanism of thermally induced motion of the domain wall in the AF/S bilayer is completely analogous to the F/S bilayer.

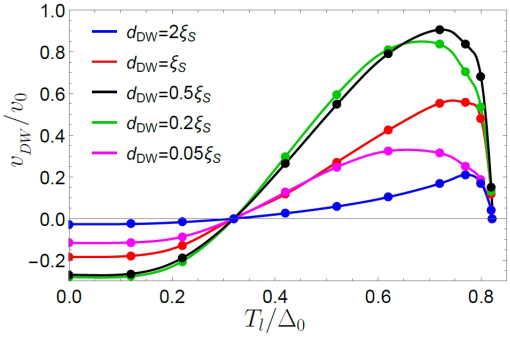

Figure 11: Domain wall velocity as a function of T_l at $T_r = 0.32\Delta_0$ for different DW widths.

The domain wall velocity in the AF/S bilayer as a function of the hot end temperature at a fixed cold end temperature is shown in Fig.11. It can be seen that the velocity vanishes in the absence of a temperature difference, which is explained by the absence of thermospin pumping in this case. Also, the velocity vanishes at a sufficiently high temperature of the hot end, which is explained by the suppression of superconductivity, which, in turn, again leads to the suppression of the thermally induced spin current. In general, the wall motion velocity is inversely proportional to the Hilbert damping parameter α. For the realistic case $\alpha = 0.01$, order of magnitude estimates give $v_0 \sim 100$ m/s for a temperature difference of 1K at the ends. For smaller values of the Hilbert damping coefficient $\alpha \sim 10^{-4}$, which are realized in yttrium-iron garnet (ferrimagnetic insulator), the velocity estimate increases by two orders of magnitude. This is a very highly efficient conversion of heat into motion of a magnetic defect. The efficiency of thermally induced motion can be characterized by the value $v_{DW}/\Delta T$, i.e. the ratio of the velocity to the applied temperature difference. In experiments on thermally induced motion of domain walls in ordinary ferromagnets [19, 20] the values $v_{DW}/\Delta T \sim 10^{-2} - 10^{-1} mm^2/Ks$ were obtained, while our estimates give $v_{DW}/\Delta T \sim 10 - 10^2 mm^2/Ks$. The results of this section were co-authored with G.A. Bobkov, A.M. Bobkov, Wolfgang Belzig and Akashdeep Kamra and published in papers **[P9]-[P10]** from the author's list of publications on the topic of the dissertation.

Third chapter is devoted to the study of magnetoelectric effects in superconducting structures containing materials with spin-orbit interaction or 3D topological insulators. Combining these materials in one chapter is due to the fact that, from the point of view of magnetoelectric effects, a 3D topological insulator looks simply like a material with the strongest spin-orbit interaction of the Rashba type. As a brief literature introduction, some known magnetoelectric effects in non-superconducting systems and their analogs in superconducting materials and structures are discussed.

In section **3.1**, a generalization of the quasiclassical theory is developed, which makes it possible to describe magnetoelectric effects in superconductor/normal metal structures with spin-orbit interaction in the ballistic limit. The essence of this generalization is that it allows one to calculate Green's functions up to the first order in the parameter $\Delta_{so}/\varepsilon_F$. Here Δ_{so} is the value of the spin-orbit splitting of the electronic spectra in the material. And this, in turn, makes it possible to describe magnetoelectric effects and triplet correlations induced by the proximity effect and SOC, while the quasiclassical approximation gives Green's functions only in the zeroth order in the parameter $\Delta_{so}/\varepsilon_F$ and does not describe this physics.

The Hamiltonian of a singlet superconductor in the presence of a general spin-orbit interaction linear in momentum can be written as [21, 22]:

$$\hat{H} = \int d^2\boldsymbol{r}' \hat{\Psi}^\dagger(\boldsymbol{r}') \hat{H}_0(\boldsymbol{r}') \hat{\Psi}(\boldsymbol{r}') + \Delta(\boldsymbol{r}) \Psi^\dagger_\uparrow(\boldsymbol{r}) \Psi^\dagger_\downarrow(\boldsymbol{r}) + \Delta^*(\boldsymbol{r}) \Psi_\downarrow(\boldsymbol{r}) \Psi_\uparrow(\boldsymbol{r}), \tag{5}$$

$$\hat{H}_0(\boldsymbol{r}) = \frac{\hat{\boldsymbol{p}}^2}{2m} - \frac{1}{2} \hat{\boldsymbol{A}} \hat{\boldsymbol{p}} - \hat{h}(\boldsymbol{r}) + V_{imp}(\boldsymbol{r}) - \mu, \tag{6}$$

where $\Delta(\boldsymbol{r})$ is the superconducting order parameter and $\hat{H}_0$ is the Hamiltonian of a normal metal in the presence of spin-orbit interaction (NSO). An arbitrary spin-orbit interaction linear in momentum is expressed by the term $\frac{1}{2}\hat{\boldsymbol{A}}\hat{\boldsymbol{p}} = \frac{1}{2} A^\alpha_j p_j \hat{\sigma}^\alpha$, where $\hat{\sigma}^\alpha$ is the Pauli matrix in spin space. $\hat{\Psi} = (\Psi_\uparrow, \Psi_\downarrow)^T$, μ is the chemical potential, and $\hat{h} = h^\alpha \hat{\sigma}^\alpha$ exchange field. We assume that the system can contain short-range nonmagnetic impurities $V_{imp}(\boldsymbol{r}) = \sum\limits_{\boldsymbol{r}_i} V_i \delta(\boldsymbol{r} - \boldsymbol{r}_i)$.

The generalized Eilenberger equation obtained in the dissertation has the form:

$$i\boldsymbol{v}_F\boldsymbol{\nabla}\check{g}+\left[\varepsilon\hat{\tau}_z+\check{\Delta}(\boldsymbol{r})+\frac{1}{2}\hat{\boldsymbol{A}}\boldsymbol{p}_F,\check{g}\right]+\frac{p_y}{4v_{F,x}}\left[\hat{A}_x,\hat{A}_y\right]\left(\check{g}^q-\mathrm{sgn}v_{F,x}\right)+\frac{i\hat{A}_yp_y}{2p_{F,x}}\partial_x\check{g}^q=0 \tag{7}$$

The third and fourth terms of this equation are not contained in the standard Eilenberger equation and are responsible for proximity-induced triplet correlations at the NSO/S interface, as well as the direct magnetoelectric effect in ballistic heterostructures. The resulting generalized Eilenberger equation must be supplemented with the generalized normalization condition

$$\check{g}^2-\frac{\hat{A}_yp_y\mathrm{sgn}v_{F,x}}{p_{F,x}v_{F,x}}\left[\check{g}^q-\mathrm{sgn}v_{F,x}\right]=1 \tag{8}$$

and generalized boundary conditions, which for an absolutely transparent boundary have the form:

$$\check{g}^l-\check{g}^r=\pm\left\{\mathrm{sgn}v_{F,x}-\check{g}^q,\frac{\hat{A}_yp_y}{4v_{F,x}p_{F,x}}\right\}, \tag{9}$$

where $\pm$ signs correspond to NSO/S and S/NSO boundaries. It can be seen that neglecting the right side of the equation (9), which is of the first order in $\Delta_{so}/\varepsilon_F$, we obtain the well-known quasiclassical boundary condition at a completely transparent interface: $\check{g}^{l,q}=\check{g}^{r,q}=\check{g}^q$, i.e. continuity of the quasiclassical Green's function. This value of the quasiclassical Green's function at the interface enters the right side of the boundary condition (9).

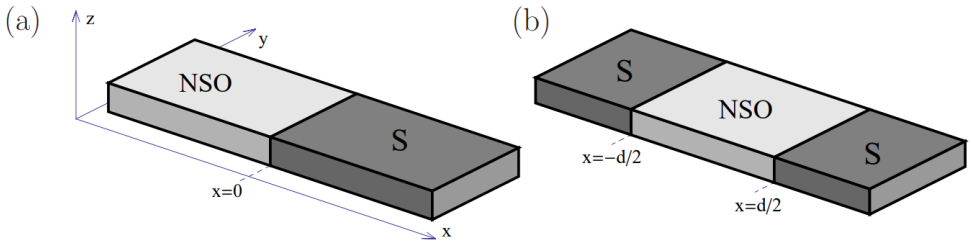

Figure 12: Sketches of (a) superconductor/normal metal bilayer with spin-orbit interaction (S/NSO) and (b) Josephson S/NSO/S junction.

Further, on the basis of the developed theory, the anomalous Green's function is calculated in the structures shown in Fig. 12. It is shown that a singlet-triplet conversion occurs at the interface of a superconductor with a spin-orbit material (S/NSO), which results in both s-wave and p-wave triplet correlations. The first type of correlations is resistant to impurity scattering, which means that it is also preserved in the dirty case. The amplitude of triplet correlations is of the first order in the $\Delta_{so}/\varepsilon_F$ parameter. In the Josephson junction shown in Fig. 12(b), these correlations lead to current-induced spin polarization of conductivity electrons (direct magnetoelectric effect). For the case of the Rashba spin orbit coupling, this polarization has the form:

$$\boldsymbol{S}=\kappa\left[\boldsymbol{c}\times\frac{\boldsymbol{j}_s}{ev_F}\right], \tag{10}$$

where j_s is the supercurrent density. For the case $\alpha p_F/2\pi T = \Delta_{so}/2\pi T \gg 1$

$$\kappa = \frac{\alpha p_F}{8\varepsilon_F}. \tag{11}$$

It is worth noting that the expressions (10) and (11) coincide with the answers obtained in [23] for the case of a ballistic homogeneous superconductor with Rashba's spin-orbit interaction. But in our case, instead of a supercurrent passing through a homogeneous material, the spin polarization is proportional to the Josephson current. The results of this section were obtained in collaboration with A.M. Bobkov and published in **[P11]** from the author's list of publications on the topic of the dissertation.

In section **3.2**, a nonequilibrium generalization of the quasiclassical theory for hybrid structures with 3D topological insulators is developed, as well as a generalization of the quasiclassical theory for superconductivity in the surface states of the 3D TI, induced by proximity to the conventional superconductor. These theories are applied to consider a number of physical effects: an anomalous phase shift in S/3D TI/S Josephson junctions without a ferromagnet, giant magnetoelectric effect in the density of states and dynamic control of magnetic anisotropy in S/F-3D TI/S Josephson junctions.

Subsection **3.2.1** is devoted to the development of a nonequilibrium generalization of the quasiclassical theory [24] for superconducting systems in which the Hamiltonian of the normal state coincides with the Hamiltonian of the conducting surface state of a 3D topological insulator. Based on this theory, an expression was obtained for the polarization of the 3D TI surface conductivity electrons induced by the flow of a supercurrent (direct magnetoelectric effect)

$$\boldsymbol{S} = \frac{1}{2e\alpha}[\boldsymbol{n} \times \boldsymbol{j}], \tag{12}$$

where $\boldsymbol{n}$ - is the normal to the 3D TI surface, α - is the Fermi velocity of the electrons in the 3D TI surface state.

Further, the nonequilibrium theory is used to solve the problem of the anomalous phase shift of the ground state of the Josephson junction via 3D TI. In this problem, the anomalous phase shift is induced and controlled by quasiparticle injection into the weak link region. The sketch of the structure under consideration is shown in Fig. 13. Taking into account the

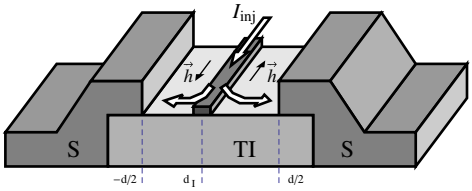

Figure 13: Sketch of a Josephson junction via 3D TI, in which a ϕ_0 junction can be realized via quasiparticle injection. The injector is at $x = d_I$ and the S/TI interfaces are at $x = \pm d/2$. The quasiparticle current (shown by the arrows) is controlled by the voltage between the injector and the superconducting terminals.

electron-electron interaction in the Hartree-Fock approximation, it is shown that quasiparticle injection creates an effective exchange field $h \propto V$ in the 3D TI surface states in the weak link region, where V is the injection voltage applied between the injector and 3D TI. In the structure under consideration, two domains are generated with opposite orientations of the effective Zeeman field, which are locked to the directions of the injected currents. This

effective Zeeman field can be written as:

$$h_y(x) = \begin{cases} -h & , \quad -d/2 < x < d_I \\ +h & , \quad d_I < x < +d/2 \end{cases} . \tag{13}$$

Next, the current-phase relation of the system under consideration is calculated. The ground state of the Josephson junction corresponds to zero current and is reached at a nonzero phase difference between superconductors $\phi_0 = \chi = -4d_I h/\alpha$. This anomalous phase shift is proportional to the voltage V between the superconducting electrodes and the injector. Therefore, in this case, the anomalous phase difference ϕ_0 can be controlled by changing this voltage. The results of this subsection were obtained in collaboration with A.M. Bobkov, A.A. Zyuzin and Muhammad Alidoust and published in **[P12]** from the author's list of publications on the topic of the dissertation.

In subsection **3.2.2**, a microscopic theory of superconductivity induced in the 3D TI surface states is developed. It is shown that the Eilenberger equation for the quasiclassical Green's function of electrons in 3D TI in a thin-film 3D TI/S bilayer has the form

$$-iv_F \boldsymbol{n}_F \boldsymbol{\nabla} \hat{g}^R = \Big[(\tilde{\varepsilon} + \tilde{\boldsymbol{h}}\boldsymbol{n}_\perp)\tau_z - \hat{\tilde{\Delta}} + \frac{i\langle \hat{g} \rangle}{2\tau}, \hat{g}\Big] \tag{14}$$

This equation has the same form as the usual Eilenberger equation for a material with a normal Hamiltonian of the 3D TI and singlet pairing, but both the quasiparticle energy term and the exchange energy are renormalized by tunnel self-energy parts that are diagonal in particle-hole space:

$$\tilde{\varepsilon} = \varepsilon + \frac{t^2}{4|v_{F,z}(\boldsymbol{p}_F)|}\Big[\frac{\varepsilon - \frac{(\boldsymbol{\nabla}\chi)\boldsymbol{p}}{2m_S} + h}{\sqrt{\Delta^2 - (\varepsilon - \frac{(\boldsymbol{\nabla}\chi)\boldsymbol{p}}{2m_S} + h)^2}} + \frac{\varepsilon - \frac{(\boldsymbol{\nabla}\chi)\boldsymbol{p}}{2m_S} - h}{\sqrt{\Delta^2 - (\varepsilon - \frac{(\boldsymbol{\nabla}\chi)\boldsymbol{p}}{2m_S} - h)^2}}\Big], \tag{15}$$

$$\tilde{\boldsymbol{h}} = \boldsymbol{h} + \frac{t^2}{4|v_{F,z}(\boldsymbol{p}_F)|}\Big[\frac{\varepsilon - \frac{(\boldsymbol{\nabla}\chi)\boldsymbol{p}}{2m_S} + h}{\sqrt{\Delta^2 - (\varepsilon - \frac{(\boldsymbol{\nabla}\chi)\boldsymbol{p}}{2m_S} + h)^2}} - \frac{\varepsilon - \frac{(\boldsymbol{\nabla}\chi)\boldsymbol{p}}{2m_S} - h}{\sqrt{\Delta^2 - (\varepsilon - \frac{(\boldsymbol{\nabla}\chi)\boldsymbol{p}}{2m_S} - h)^2}}\Big]\frac{\boldsymbol{h}}{h}. \tag{16}$$

The phenomenological order parameter is also replaced by the effective order parameter $\hat{\tilde{\Delta}}$, which comes from the wave function of the superconductor Cooper pairs and has the form:

$$\tilde{\Delta} = \frac{t^2}{4|v_{F,z}(\boldsymbol{p}_F)|}\Bigg[\Big(\frac{\Delta}{\sqrt{\Delta^2 - (\varepsilon - \frac{(\boldsymbol{\nabla}\chi)\boldsymbol{p}}{2m_S} + h)^2}} + \frac{\Delta}{\sqrt{\Delta^2 - (\varepsilon - \frac{(\boldsymbol{\nabla}\chi)\boldsymbol{p}}{2m_S} - h)^2}}\Big) + \Bigg[\Big(\frac{\Delta}{\sqrt{\Delta^2 - (\varepsilon - \frac{(\boldsymbol{\nabla}\chi)\boldsymbol{p}}{2m_S} + h)^2}} - \frac{\Delta}{\sqrt{\Delta^2 - (\varepsilon - \frac{(\boldsymbol{\nabla}\chi)\boldsymbol{p}}{2m_S} - h)^2}}\Big)\frac{\boldsymbol{h}\boldsymbol{n}_\perp}{h}\Bigg]. \tag{17}$$

This subsection shows that, within the framework of the phenomenological model with singlet pairing, the supercurrent passing through the 3D TI surface state is completely equivalent to the action of the Zeeman field $\boldsymbol{H}_{eff} = (-v_F(\partial_y\chi)/2, v_F(\partial_x\chi)/2, 0)$. This field is generated by a supercurrent that corresponds to the phase gradient of the order parameter $\boldsymbol{\nabla}\chi$ and is perpendicular to it. This is a remarkable property of helical metal, which underlies a large number of bright magnetoelectric effects. Within the considered microscopic model, the complete equivalence between the Zeeman term and the supercurrent is lost. This is because there is no such equivalence in a superconductor that is not a helical metal. However, at

low energies $\varepsilon, H_{eff} \ll \Delta$ in zero order in the parameter $(\varepsilon, H_{eff})/\Delta$, our microscopic model reduces to a phenomenological one with $\tilde{\varepsilon} \to \varepsilon$, $\tilde{h} \to h$ and the induced order parameter $\tilde{\Delta}_{\varepsilon\to 0} \approx t^2/2|v_{F,z}|$. In this low energy region, the equivalence between the Zeeman term and the supercurrent is preserved.

It is also shown in subsection **3.2.2** that such an equivalence leads to the appearance of a spin splitting of the density of states of electrons in the superconducting surface state of a topological insulator, which is similar to the spin splitting of the density of states of a BCS superconductor in a Zeeman field. This effect is called giant magnetoelectric. The supercurrent-induced spin splitting of the density of states is shown in Fig. 14. This

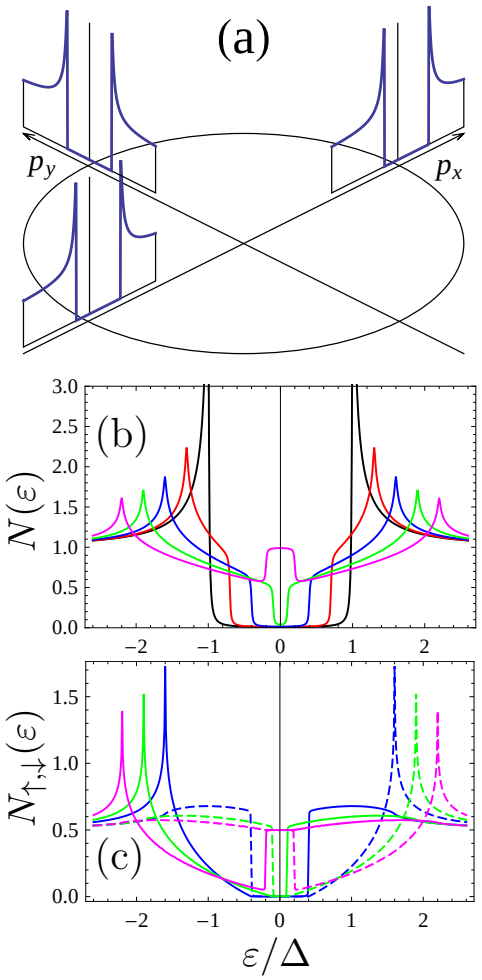

Figure 14: DOS for the ballistic system. (a) Momentum-resolved DOS. The circle shows the Fermi surface, and for each direction of the momentum, its own energy axis is introduced, which is directed outside the circle and normal to it. (b) Momentum-averaged DOS as a function of quasiparticle energy. $H_{eff}/\Delta = 0$ (black line); 0.3 (red); 0.6 (blue); 0.9 (green); 1.2 (pink). (c) Spin-resolved DOS as a function of the quasiparticle energy. $H_{eff}/\Delta = 0.6$ (blue); 0.9 (green); 1.2 (pink). The quantization axis is directed along the y axis, and $\boldsymbol{j}_s = j_s\hat{x}$. The DOS for spin up $N_\uparrow$ is shown with solid lines, and the DOS for spin down $N_\downarrow$ is shown with dashed lines.

effect can be used to spin filter the electric current through an additional tunnel junction. In this case, both the magnitude of the spin polarization of the tunneling current and its direction are controlled by the magnitude and direction of the supercurrent flowing through

the superconductor. The results of this subsection were obtained in collaboration with A.M. Bobkov and published in **[P13]** from the author's list of publications on the topic of the dissertation.

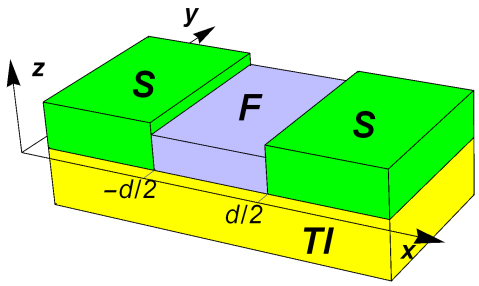

Figure 15: Sketch of the system considered in subsection **3.2.3**. Superconducting leads and a ferromagnetic weak link are placed on a 3D TI surface.

In subsection **3.2.3**, the effect of dynamic control of magnetic anisotropy in Josephson junctions through a combined weak link consisting of a bilayer of a topological insulator and a ferromagnetic metal is studied. The sketch of the system is shown in Fig. 15. It is shown that in Josephson S/F/S junctions lying on 3D TI, the anomalous phase shift also causes magnetization dynamics, as in spin-orbit systems. However, in contrast to systems with spin-orbit interaction, where the dynamics of the magnetization has already been studied earlier, for our system, not only the anomalous phase shift, but also the critical current strongly depends on the orientation of the weak link magnetization. Namely, it depends only on the magnetization component lying in the surface plane TI and directed along the current. We show that such a dependence under the conditions of the nonstationary Josephson effect at a given voltage applied to the junction can lead to splitting of the easy axis of the magnet. The choice of voltage makes it possible to dynamically stabilize a fourfold degenerate ferromagnetic state in a ferromagnet, which under equilibrium conditions is an easy-axis ferromagnet.

Stationary magnetization points correspond to $m_z = \pm 1$ or $m_z = 0$. Stationary points $m_z = \pm 1$ are always unstable. The dissertation shows that 4 stable points $\boldsymbol{m}^{st} = (\pm|m_x^{st}|, \pm|m_y^{st}|, 0)$ appear in a certain range of system parameters. The physical reason for this is that, as a result of the locking between the electron momentum and its spin, the critical current of the system is suppressed only by the m_x magnetization component (along the current). Therefore, it is favorable for the system to have a nonzero m_x component to minimize the Josephson energy. The competition of this contribution to the energy and magnetic anisotropy energies along the y axis leads to the stabilization of new dynamic equilibrium positions.

Fig. 16 shows the complete temporal evolution of the magnetization $\boldsymbol{m}$ obtained from the numerical solution of the LLG equation. It can be seen that starting from different initial conditions, it is possible to get into all 4 stable equilibrium positions. The results were obtained in collaboration with A.M. Bobkov, M. Nashaat, Yu.M. Shukrinov, I.R. Rakhmonov and K. Sengupta and published in **[P14]** from the author's list of publications on the topic of the dissertation.

Section **3.3** predicts and investigates a new type of long-range interaction of magnetic moments in a system of coupled Josephson junctions, the physical basis of which is the magnetoelectric interaction of the magnetic moment with the condensate phase (inverse magnetoelectric effect). The considered type of interaction is not based on proximity effects

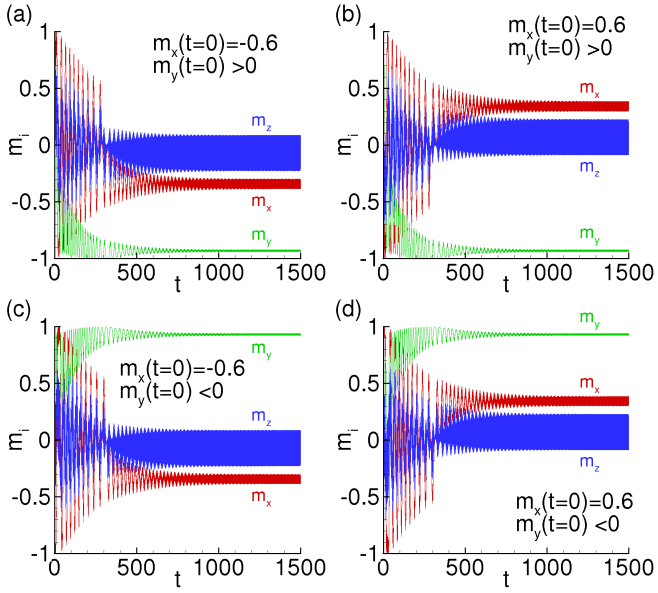

Figure 16: Time evolution of magnetization starting from different initial conditions. (a) $m_x(t=0) = -0.6$, $m_y(t=0) = 0.8$, (b) $m_x(t=0) = 0.6$, $m_y(t=0) = 0.8$, (c) $m_x(t=0) = -0.6$, $m_y(t=0) = -0.8$ and (d) $m_x(t=0) = 0.6$, $m_y(t=0) = -0.8$. For all panels $m_z(t=0) = 0$. 4 panels correspond to 4 possible stationary states that can be reached by the system at large t. $\Gamma = 1.57$, $r = 0.5$, $\tilde{d} = 0.3$, $\alpha = 0.01$, $\Omega_F/\Omega_J = 0.2$, time is measured in units of Ω_J^{-1}.

in a superconductor, and therefore is not limited by the coherence length or the penetration depth of the magnetic field. The interaction mechanism is based on the fact that superconductivity is a macroscopic quantum phenomenon with a single condensate phase, and the condensate phase is related to the magnetization of magnets through the magnetoelectric effect. The energy of the ground state of a system of two coupled Josephson S/F/S junctions at a given phase difference between the outer superconducting leads depends on the mutual orientation of the magnets forming weak links, which means the interaction between them.

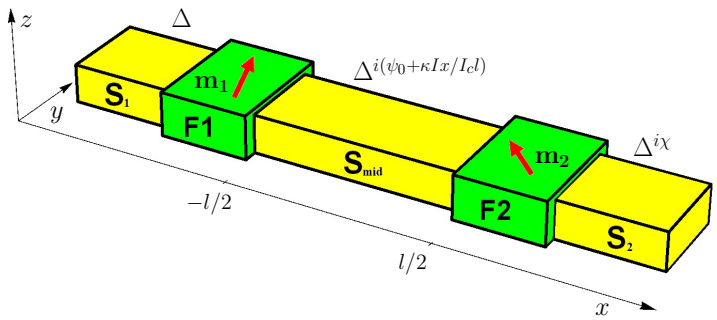

Figure 17: Sketch of a system of coupled S/F/S Josephson junctions.

We assume that the discussed effect can be observed in systems where there is a magnetoelectric coupling between the magnetization direction of the magnet and the Josephson phase. It is known that such a coupling physically manifests itself as an anomalous phase

shift in the ground state of the Josephson junction. Therefore, we consider a system consisting of two coupled Josephson S/F/S junctions, where S is a conventional singlet s-wave superconductor, and F is a ferromagnetic weak link of a Josephson junction, in which spin-orbit interaction is also present. The scheme of the system is shown in Fig. 17.

The energy of the system is calculated as a function of the phase difference χ between the outer superconducting leads. Near the minima, it has the form:

$$E \approx -\frac{2E_J r(m_{y1}+m_{y2})\tilde{\chi}}{(2+\kappa)^2} + \frac{E_J r^2(m_{y1}^2+m_{y2}^2)}{(2+\kappa)^2} + \frac{2E_J r^2 m_{y1}m_{y2}}{(2+\kappa)^2} - E_M(m_{y1}^2+m_{y2}^2) + const. \quad (18)$$

The first term in Eq. (18) describes the individual interaction of the magnetic moments with the phase, the second term works as an additional contribution to the magnetic anisotropy energy, and the third term describes the interaction between the moments. The interaction constant is $J_{eff} = 2E_J r^2/(2+\kappa)^2 > 0$, and hence the interaction has an antiferromagnetic character. At large external phases χ, the first term dominates, leading to the fact that the ground state will be $\uparrow\uparrow$ or $\downarrow\downarrow$, but at smaller phases, the antiferromagnetic interaction overcomes the individual interaction of moments with the phase. The spatial dependence of J_{eff} is determined by $\kappa \propto l$, i.e. $J_{eff} \propto l^{-2}$ for large l. To estimate $\kappa \sim eI_c l/\sigma_S \Delta S$, where Δ is the superconducting order parameter, σ_S is the conductivity of the average superconductor in the normal state, and S is its cross section, we take the typical parameters $Nb/Bi_2Te_3/Nb$ Josephson junctions $I_c = w \cdot [40A/m]$, where $w \sim 1\mu m$ is the junction width along the y-direction, $\sigma_S = \sigma_{Nb} = 10^7(\Omega \cdot m)^{-1}$, $\Delta_{Nb} = 2.5 \cdot 10^{-22}$J and $S = (1\mu m)^2$. Then $\kappa \sim 1$ for $l \sim 1mm$. Thus, these estimates show that the interaction strength practically does not change with distance up to the submillimeter range. Moreover, if the length of the middle superconductor reaches $\sim 1mm$, the inductance energy $E_L = LI^2/2$ already becomes of the same order as the Josephson energy and should be taken into account. Accounting for this energy leads to the need to make the substitution $E_J \to E_J + LI_c^2/2$ in the equation (18). Because $L \propto l$, this modifies the decay law of the interaction constant between magnets $J_{eff} \propto l^{-1}$ at large distances between them.

The coupled dynamics of magnetic moments in such a system is also studied. The possibility of remote switching of the magnetic moment is demonstrated. The results were obtained in collaboration with G.A. Bobkov and A.M. Bobkov and published in **[P15]** from the author's list of publications on the topic of the dissertation.

Section **3.4** is devoted to the study of the magnetoelectric effect, which is possible only in superconducting hybrid systems - the generation of triplet superconductivity by the condensate motion. The physical principle of the effect is described, the theory of triplet superconductivity induction by Meissner currents, as well as dynamic superconductivity by an alternating electromagnetic field, is developed. Possible applications of the effect for spintronics and superconducting electronics are discussed: Josephson transistor, photomagnetic element, $0-\pi$ supercurrent-controlled junction. The results were obtained in collaboration with A.M. Bobkov, M.A. Silaev and A.A. Mazanik and published in papers **[P16]-[P18]** from the author's list of publications on the topic of the dissertation.

In subsection **3.4.1** it is shown that the motion of a superconducting condensate, which is generated by an external magnetic field through the Meissner effect, makes it possible to generate triplet odd-frequency superconductivity in existing SOC structures. In the context of S/F hybrid structures, these correlations are known as long-range triplet correlations (LRT) because they penetrate into a ferromagnetic material over relatively large distances

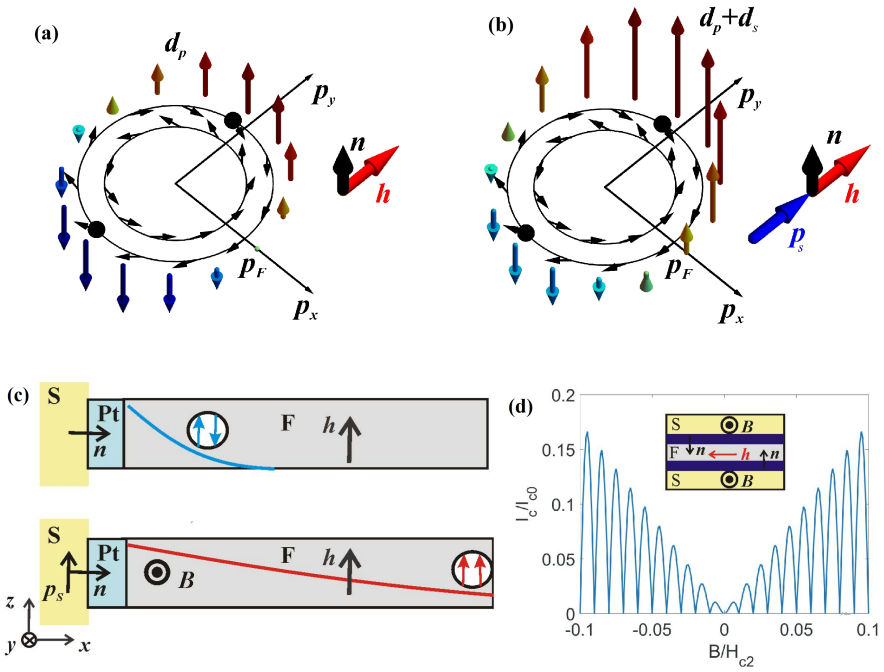

Figure 18: (a)-(b) Mechanism of formation of s-wave spin-triplet superconducting correlations. (c) Scheme of an S/F system with a Rashba-type SOC at the interface, which is generated by a thin layer of Pt heavy metal. In the absence of a magnetic field, only rapidly decaying triplet correlations are generated. The magnetic field generates the motion of condensate through the Meissner effect $\boldsymbol{p}_s = -(\lambda_L/\Phi_0)\boldsymbol{n}\times\boldsymbol{B}$. The interaction of the condensate momentum $\boldsymbol{p}_s$, SOC, and the exchange field $\boldsymbol{h}$ leads to the appearance of a weakly decaying s-wave triplet component for $\boldsymbol{B} \neq 0$. (d) Interference pattern of the critical current $I_c(\Phi)$ for the magnetic field-induced Josephson effect in the junction shown in the inset.

of the order of the superconducting coherence length in a normal metal [12]. The scheme of the considered S/F interface is shown in Fig. 18(c).

The qualitative physics of the effect can be explained as follows. A thin Pt layer at the S/F interface where a Rashba-type SOC is present can be considered as a quasi-2D superconductor (superconductivity is induced in it by the proximity effect with the superconductor) in an effective exchange field induced by the proximity effect with the ferromagnet. Triplet pairs of electrons with equal spins are generated in this thin layer and then penetrate the ferromagnet where they are LRTs. SOC does not lead to the destruction of spin-singlet and, generally speaking, any pairs of electrons with opposite spins. This can be illustrated using the Rashba-type SOC metal system model, which is described by the Hamiltonian $\hat{H} = \xi_p + \alpha(\boldsymbol{p}\times\boldsymbol{n})\cdot\boldsymbol{\sigma}$, where $\xi_p = p^2/2m - \varepsilon_F$ is the kinetic energy of an electron relative to the Fermi level ε_F. The presence of SOC in this Hamiltonian leads to the formation of helical subbands. In these subbands, the spin quantization axis $\parallel (p_y, -p_x)$ depends on the direction of the momentum. However, these axes are still collinear for electrons with opposite momenta $\boldsymbol{p}$ and $-\boldsymbol{p}$. Therefore, in such a system, the superconducting state can be formed by ordinary spin-singlet pairs, provided that the spin splitting of the Fermi surfaces is small, which is a typical situation for a surface SOC.

Let now an exchange field be applied to the system, for example, directed perpendicular to the vector $\boldsymbol{n}$: $\boldsymbol{h} = h\boldsymbol{y}$. In this case, the spin quantization axes for electrons with $\boldsymbol{p}$ and $-\boldsymbol{p}$ are no longer collinear, see Fig. 18(a). Therefore, pure spin-singlet pairing is no

longer possible. Spin-triplet correlations appear, which are characterized by the spin vector $\boldsymbol{d}_p(\boldsymbol{p},\omega) = F_{pw}(\omega)\boldsymbol{h}\times(\boldsymbol{n}\times\boldsymbol{p})$ with amplitude $F_{pw}(\omega)$. A typical spin vector texture $\boldsymbol{d}_p$ is shown in Fig. 18(a). This state corresponds to p-pairing, because the wave function is an odd function of the electron momentum $\boldsymbol{d}_p(\boldsymbol{p}) = -\boldsymbol{d}_p(-\boldsymbol{p})$. Condensate motion is the third ingredient needed to generate LRT. The nonzero momentum $\boldsymbol{p}_s$ of the condensate leads to mixing of the p-wave and s-wave components of the condensate. The Doppler shift leads to a shift in the Matsubara frequencies. As a result the triplet correlation amplitude becomes $F_{pw}(\omega - i\boldsymbol{v}_F\cdot\boldsymbol{p}_s) \approx F_{pw}(\omega) - i(\boldsymbol{v}_F\cdot\boldsymbol{p}_s)\partial_\omega F_{pw}$. This modification of the pair amplitude produces an additional s-wave component of the spin vector $\boldsymbol{d}_s = \langle\boldsymbol{d}_p(\boldsymbol{p},\omega - i\boldsymbol{v}_F\boldsymbol{p}_s)\rangle \approx (2/3i)\varepsilon_F(\partial_\omega F_{pw})\boldsymbol{h}\times(\boldsymbol{n}\times\boldsymbol{p}_s)$, where the angle brackets denote the averaging over the directions of the electron momentum on the Fermi surface. The vector field $\boldsymbol{d} = \boldsymbol{d}_p + \boldsymbol{d}_s$, where $\boldsymbol{d}_s \propto \boldsymbol{h}\times(\boldsymbol{n}\times\boldsymbol{E})$ is schematically shown in Fig. 18 (b), where the configuration with $\boldsymbol{p}_s \parallel \boldsymbol{h} \perp \boldsymbol{n}$ is considered, which gives $\boldsymbol{d} \parallel \boldsymbol{n}$ and mixes p-wave and s-wave pairing, what leads to $|\boldsymbol{d}(\boldsymbol{p})| \neq |\boldsymbol{d}(-\boldsymbol{p})|$.

For the upper structure shown in Fig. 18(c) with $\boldsymbol{B} = 0$, we have $\boldsymbol{d}_s = 0$ and thus, despite the presence of SOC, only Cooper pairs with $S_z = 0$ exist. Such correlations in a diffuse ferromagnet decay at distances on the order of the magnetic coherence length $\xi_F = \sqrt{D/h}$, which is quite short - $\xi_F \sim 1$ nm in conventional ferromagnetic metals. Therefore, with exponential accuracy, superconductivity is absent at distances $x \gg \xi_F$ from the S/F interface. At the same time, correlations with $\boldsymbol{d}_s \neq 0$ that appear at $\boldsymbol{B} \neq 0$ have $S_z = \pm 1$. Therefore, they are LRTs that are resistant to spin depairing by the exchange field and are preserved in the ferromagnet at distances $x \gg \xi_F$ from the S/F interface. In the structure shown in Fig. 18(c), such pairs appear only after the application of a magnetic field $\boldsymbol{B} \perp \boldsymbol{h}$. Therefore, we can speak about the mechanism of generation of triplet superconductivity by a magnetic field. The formation of LRTs is essential for the transport properties of the system, which can be measured directly. The dissertation discusses two of them - tunnel conductance and Josephson current.

The critical Josephson current S/F/S of a contact with spin-orbit interfaces as a function of the applied magnetic field is shown in Fig. 18(d). The physical origin of the unusual behavior of the critical current oscillations depending on the applied magnetic field is determined by the mechanism of LRT generation by the magnetic field. The LRT amplitude is proportional to the condensate momentum $\boldsymbol{p}_s$, which is generated by an external magnetic field through the Meissner effect. Near the S/F interfaces $x = \pm d_F/2$ we have $p_s = \mp\lambda_L B_0/\Phi_0$. Consequently, the critical current amplitude grows as $I_c \propto B^2$ for small values of the applied field, when the total flux through the junction area $\Phi = 2\lambda_L L B$ is small, $\Phi \ll \Phi_0$. Here L is the junction length along the S/F interfaces. For large fields, we must take into account the change along the S/F interface, which leads to the usual factor $(L\sin\phi)/\phi$ at the critical current, where $\phi = 2\pi\Phi/\Phi_0$. As a result, we find that the critical current as a function of the field oscillates as usual, but the envelope of these oscillations grows linearly with the field $I_c \propto B$. This growth is limited from above by depairing effects, of which the most important is the entry of the vortex into the superconducting leads, caused by the external magnetic field B. This occurs at fields of the order of H_v, when the momentum of the condensate at the edges of the superconductor reaches the critical depairing value $p_s\xi \sim 1$. Depending on the strength of disorder, you can get $H_v/H_{c2} \sim 0.1 - 0.19$. It is in this range of fields that Fig. 18(d) is plotted.

In subsection **3.4.2**, dynamical triplet states are studied, which are generated by external alternating electric fields. From the point of view of physics, this effect is close to that considered in the previous subsection, because again triplet superconductivity is induced by

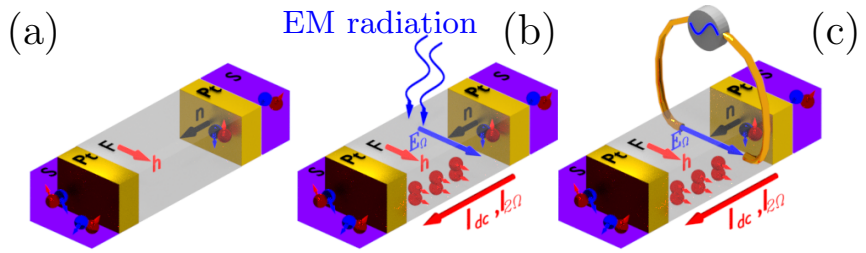

Figure 19: S/F junction with Rashba type SOC at the S/F interface, which is created by a thin layer of Pt. (a) In the ground state of the junction, only short-range triplet correlations are present, shown as blue and red balls with opposite spins. (b,c) Generation of LRTs by irradiating the system with an electromagnetic field (b) or an alternating current source (c). In both cases, an electric field $\boldsymbol{E}(t) = \boldsymbol{E}_\Omega e^{i\Omega t}$ is created in the ferromagnetic weak link. LRTs are shown schematically as red balls with unidirectional arrows, which correspond to spin states codirectional with the exchange field $\boldsymbol{h}$.

the condensate motion, but now this motion is caused by the application of an alternating electromagnetic field, rather than a constant magnetic one. In addition to being of fundamental interest, the effect opens up the possibility of controlling the Josephson current by high-frequency fields. This mechanism makes it possible to achieve switching rates in the terahertz and even visible frequency range.

It is shown that an external alternating electric field induces triplet correlations, the spin vector of which is constructed as follows:

$$\boldsymbol{d}(\varepsilon, t) = \int dt' K_d(\varepsilon, t - t')(\boldsymbol{E}(t') \times \boldsymbol{n}) \times \boldsymbol{h}, \tag{19}$$

where $\boldsymbol{n}$ is the normal to the S/F interface plane. As usual, the spin vector $\boldsymbol{d}$ depends on the quasiparticle energy ε. However, the problem under consideration is essentially nonstationary and therefore it also depends on time. The scalar kernel $K_d(\varepsilon, t-t')$ is determined by the details of the microscopic model. The scale of nonlocality in time is determined by the characteristic frequencies of the response of the superconducting condensate to an alternating field. Possible schemes of systems in which the effect can be realized are shown in Fig. 19. In the case where the long-range proximity effect is caused by a harmonic electromagnetic wave, the current-phase relation is:

$$I(\chi, t) = [I_{dc}^c + I_{2\Omega}^c \cos(2\Omega t)] \sin\chi. \tag{20}$$

That is, the critical current has a dc component $I_{dc}^c \propto E_\Omega E_{-\Omega}$ and a second harmonic $I_{2\Omega}^c \propto E_\Omega^2$.

The Josephson current induced by an electric field through JJ opens up an interesting possibility of creating photomagnetic elements based on a superconducting loop with a weak link, which is formed by a photoactive Josephson junction. The dissertation shows that by applying radiation to a system that is a dc SQUID, one of the branches of which contains a photoactive Josephson junction, and the other a regular π-contact, it is possible to induce a spontaneous current circulating in the loop, which in turn produces a constant magnetic field component $\boldsymbol{B}_{dc}$.

In subsection **3.4.3** it is shown that the effect of generating LRTs by condensate motion is not limited to hybrid systems with Rashba-type surface SOC, but exists in a much wider class

of systems with impurity spin-orbit interaction. The dissertation considers the case when the impurity spin-orbit interaction is present in the superconductor. The key parameters for generating LRT correlations in S/F systems are the spin-Hall angle θ and the spin current swapping coefficient κ. In the presence of a non-zero condensate pulse $\boldsymbol{p}_s$, each of them generates LRTs according to its own physical mechanism, which are physically different.

The spin-Hall angle is responsible for the analogue of the well-known spin Hall effect in superconducting systems. Namely, it was shown [25] that at $\theta \neq 0$ the nonzero momentum of the condensate induces triplet components of the condensate at the edges of a superconducting strip of finite width. The vector structure of the triplet wave function of the Cooper pair is defined by the normal to the edges of the strip $\boldsymbol{n}$ and the condensate momentum $\boldsymbol{p}_s$ as $\boldsymbol{f}_t \propto \boldsymbol{p}_s \times \boldsymbol{n}$. For the case under consideration, the S/F interface plays the role of edges. After entering the ferromagnetic region, the triplet pairs feel the exchange field of the ferromagnet $\boldsymbol{h}$. We choose the spin quantization axis along $\boldsymbol{h}$. Then, if $\boldsymbol{h}$ is co-directed with $\boldsymbol{p}_s \times \boldsymbol{n}$, the only nonzero component $\boldsymbol{f}_t = f_t \boldsymbol{e}_z$ is directed along the z axis. That is, triplet correlations consist of pairs with opposite spins that decay in a ferromagnet on the scale of the magnetic coherence length ξ_F [11]. As mentioned earlier, this is a very short length of the order of several nanometers in ordinary ferromagnets such as Fe or permalloy. At the same time, if $\boldsymbol{h}$ has a non-zero component perpendicular to $\boldsymbol{p}_s \times \boldsymbol{n}$ [which means that only the p_{sz} component of the condensate momentum works], the triplet correlation vector $\boldsymbol{f}_t$ is no longer co-directed with the z axis and has a component perpendicular to it, which describes pairs with equal spins. Such pairs penetrate far into a ferromagnet [12] and decay on the scale of the normal coherence length $\propto \sqrt{D_F/2\pi T_c}$, which has an order of magnitude from tens to hundreds of nanometers, depending on the material. Thus, an appropriate choice of the direction of the condensate momentum makes it possible to make triplet pairs, which are generated through the superconducting spin Hall effect, weakly decaying in a ferromagnet.

The second mechanism for generating LRTs is realized through the spin current swapping coefficient κ. It is completely different. In contrast to the previous mechanism, in the absence of an exchange field in the system, triplet pairs are not generated by this mechanism. This statement is further confirmed by direct calculations. In the presence of an exchange field, LRTs are induced in two stages. First, short-range triplets with opposite spins are generated at the S/F interface through the usual singlet-triplet conversion [11]. Then the spin of these pairs, which have a non-zero momentum due to the motion of the condensate along the interface, partially rotates through the spin current swapping mechanism [26]. In order to create LRT pairs through this mechanism, i.e. to induce a component $\boldsymbol{f}_t$ perpendicular to $\boldsymbol{h} = h\boldsymbol{e}_z$, the momentum of the condensate must again have a nonzero component along the z direction.

The dissertation carried out quantitative calculations of LRTs arising from these mechanisms. It is shown that the Josephson current carried by long-range triplet correlations for the case of absolutely transparent S/F interfaces has the form:

$$j_x(\varphi) = \frac{4\sigma}{e}\frac{|\Delta|^2}{\pi T_c}\frac{\left\{\kappa^2 + \theta^2\left(1+\frac{\xi_F}{\xi_S}\right)^2\right\}}{\left[1+\left(1+\frac{\xi_F}{\xi_S}\right)^2\right]^2}\frac{\xi_F^2}{4\xi_S}e^{-d_F/\xi_S}\left[(\mathbf{n_h}\cdot\mathbf{p}_{sR})((\mathbf{n_h}\cdot\mathbf{p}_{sL})\right]\sin\varphi. \tag{21}$$

Here $\mathbf{n_h} = \boldsymbol{h}/h$. For the case of tunnel interfaces, the corresponding expression has the form:

$$j_x(\varphi) = \frac{4\sigma_F}{e}\frac{|\Delta|^2}{\pi T_c}\frac{1}{2\sinh\frac{d_F}{\xi_{FL}}}\xi_{FL}\left(\gamma\theta\xi_S\right)^2\left[(\mathbf{n_h}\cdot\mathbf{p}_{sR})(\mathbf{n_h}\cdot\mathbf{p}_{sL})\right]\sin\varphi. \tag{22}$$

Here $\mathbf{p}_{sL(R)}$ is the momentum of the condensate in the left and right superconductors along the S/F interfaces.

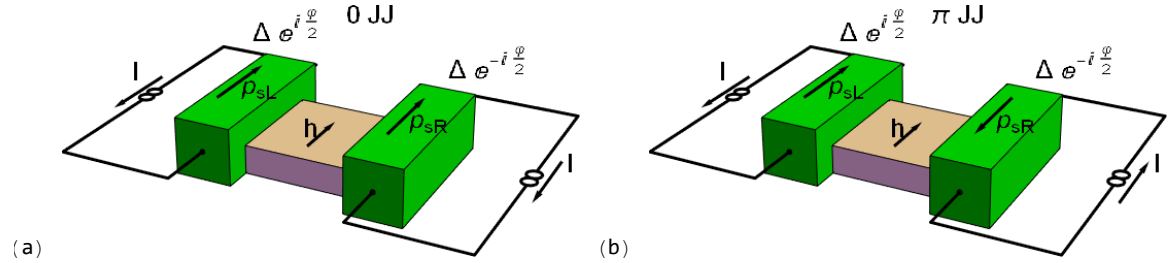

Figure 20: The principle of $0-\pi$ switching by changing the direction of condensate flow. The condensate motion is created by the supercurrent applied in the leads along the S/F interfaces. The direction of condensate motion in each of the leads can be reversed by reversing the direction of the applied supercurrent.

The condensate motion can be caused by applying an external magnetic field to the junction. If the LRT is generated by an external magnetic field, then the corresponding contact is in the π-ground state. This fact follows from the relation $p_{szL} = -p_{szR}$ between the directions of the momentum of the condensate in the superconducting leads. However, the supercurrent along the S/F interfaces can be caused not only by the magnetic field. It can be applied simply with a current source, see Fig. 20. In this case, the absolute value and direction of $\boldsymbol{p}_s$ in each lead is determined by the applied current. In particular, it is possible to switch the system between the situations $p_{szL} = p_{szR}$ and $p_{szL} = -p_{szR}$ by changing the direction of the supercurrent in one of the leads. Switching results in a controlled $0-\pi$ transition. This effect, which is interesting from the point of view of applications of superconducting electronics, is considered in subsection **3.4.4**.

The fourth chapter is devoted to the study of magnetoelectric effects in superconducting hybrids with spin-textured magnets. It is known that in a reference frame associated with a local spin basis, the spin texture is mathematically equivalent to some type of spin-orbit interaction, i.e. gauge SU(2) field $\hat{\sigma}_k M_{ki}$, where

$$M_{kj} = \frac{\mathrm{Tr}\left(\hat{\sigma}_k \hat{U}^\dagger \nabla_j \hat{U}\right)}{2im} \tag{23}$$

arises from the unitary spin transformation $\hat{U}(\boldsymbol{r}) = e^{i\boldsymbol{\sigma}\boldsymbol{\theta}(\boldsymbol{r})/2}$. The transformation matrix is parametrized by the spin vector $\boldsymbol{\theta}$, which is determined by the spatial texture of the exchange field $\boldsymbol{h}(\boldsymbol{r}) = \hat{R}(\boldsymbol{\theta}(\boldsymbol{r}))\boldsymbol{h}_0$, where $\hat{R}$ is a spatially dependent rotation matrix and we choose $\boldsymbol{h}_0 = h_0\boldsymbol{z}$. Therefore, hybrids with spin-textured magnets exhibit a very rich pattern of magnetoelectric effects.

Section **4.1** investigates the direct and inverse proximity effects in Josephson junctions with strong textured magnets. Subsection **4.1.1** shows that a superconducting condensate can sense spin-dependent gauge fields in S/F heterostructures consisting of ordinary singlet superconductors and strong ferromagnets, in which the spin subbands are substantially split by the exchange field. Quasiclassical equations are derived that describe the superconducting correlations of electrons located on the Fermi surface for spin up/down in a local spin basis (see a schematic representation of such correlations in Fig. 21(a)). These equations are written separately for electrons with spins up and down and have the form:

$$i\boldsymbol{v}_\sigma \hat{\partial}_{\boldsymbol{R}} \hat{g}_\sigma + [i\omega\hat{\tau}_3 - \hat{\Sigma}_\sigma, \hat{g}_\sigma] = 0, \tag{24}$$

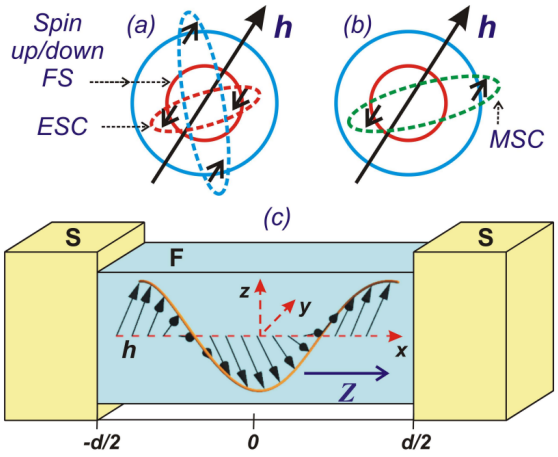

Figure 21: (a,b) Schematic representation of Cooper pairs that are formed on spin-split Fermi surfaces (FS). (a) Weakly decaying triplet equal-spin electron correlations (ESC) between electrons sitting on Fermi surfaces for spins up and down. (b) Correlations of electrons with opposite spins (MSC) that occur between electrons with different FS. (c) Josephson junction through a strong ferromagnet (F) with a magnetic helical texture producing a $\boldsymbol{Z} \parallel \boldsymbol{x}$ gauge field that generates spontaneous charge currents between the superconducting electrodes (S).

where the covariant operator

$$\hat{\partial}_{\boldsymbol{R}} = \nabla_{\boldsymbol{R}} + i\sigma \boldsymbol{Z}[\hat{\tau}_3, \cdot] - ie\boldsymbol{A}[\hat{\tau}_3, \cdot] \tag{25}$$

$$\boldsymbol{Z} = (M_{zx}, M_{zy}, M_{zz}) m_F. \tag{26}$$

Thus, it turns out that the Eilenberger equations for spin up/down electron correlations contain an additional U(1) gauge field $\boldsymbol{Z}$, which is added to the usual electromagnetic vector potential $\boldsymbol{A}$ with opposite charges for Cooper pairs with spin up/down. This U(1) field is obtained by projecting the initial SU(2) gauge field onto the spin-triplet states by taking the diagonal elements $\boldsymbol{Z} = -i(\hat{U}^{-1}\nabla\hat{U})_{11}$. This reduction means that we neglect the spin flip processes induced by the SU(2) potential. The phases acquired by spin up/down electron pairs in response to this gauge field generate spontaneous spin and charge currents through strong ferromagnets.

The current-phase relation $I = I(\chi)$ of the Josephson junction through a strong textured ferromagnet takes the form:

$$I(\chi) = \sum_{\sigma=\pm} I_\sigma \sin(\chi + 2\sigma Z_x d) \tag{27}$$

where χ is the phase difference between the superconducting leads.

In the presence of a nonzero component of the spin gauge field $Z_x \neq 0$ and broken spin degeneracy of the kinetic coefficients, i.e. $D_+ \neq D_-$ and $v_+ \neq v_-$, CPR (27) gives a spontaneous current at zero phase difference, known as the anomalous Josephson effect. The corresponding ground state phase difference χ_0 can be found from the zero current condition $I(\chi = \chi_0) = 0$

$$\tan\chi_0 = \frac{I_- - I_+}{I_- + I_+} \tan(2Z_x d). \tag{28}$$

Thus, it is shown that, in a strong ferromagnet, gauge spin fields, which are an effective description of the spin texture of a ferromagnet, lead to the generation of spontaneous supercurrents, which can be measured through the anomalous phase shift of the Josephson junction in a wide class of S/F/S structures relevant to the superconducting spintronics. The results of this subsection were obtained in collaboration with A.M. Bobkov and M.A. Silaev and published in **[P19]** from the author's list of publications on the topic of the dissertation.

In view of applications to energy-saving technologies, the study and use of spin torques caused by non-dissipative supercurrents looks quite promising. For spin-textured hybrid S/F structures, the existence of spin-polarized supercurrents is quite typical, and there they are carried by the long-range triplet component of the condensate [12]. However, earlier there was no general understanding of the physical picture of interaction between supercurrent and spin texture. For this reason the possibility of supercurrent-induced motion of domain walls and skyrmions in real ferromagnets has been an open question for a long time, despite the great attention attracted to this topic. Subsection **4.1.2** is dedicated to this important issue.

It is shown that the spin-polarized supercurrent can induce the magnetization dynamics, which is described in terms of the LLG equation

$$\dot{\boldsymbol{M}} = -\gamma \boldsymbol{M} \times \boldsymbol{H}_{eff} + \frac{\alpha}{M} \boldsymbol{M} \times \dot{\boldsymbol{M}}. \tag{29}$$

The superconducting spin current $\boldsymbol{J}$ can induce two types of spin torque, which can be written as a correction to the effective field $-\gamma \boldsymbol{M} \times \tilde{\boldsymbol{H}}_{eff} = \boldsymbol{N}_{st} + \boldsymbol{N}_{so}$. The first term is the adiabatic torque and the second term $\boldsymbol{N}_{so}$ is the spin-orbit (SO) torque:

$$\boldsymbol{N}_{st} = 2\mu_B (\tilde{\boldsymbol{J}}^z \nabla) \boldsymbol{m}, \tag{30}$$

$$\boldsymbol{N}_{so} = 4\mu_B m_F (\boldsymbol{m} \times \boldsymbol{B}_j) \tilde{J}^z_j, \tag{31}$$

where $\boldsymbol{m} = \boldsymbol{M}/M$. Here, the vector $\boldsymbol{B}_j = (B_{xj}, B_{yj}, B_{zj})$ is introduced, which is determined by the j-th coordinate component of the tensor $\hat{B}$, which describes an arbitrary linear in momentum spin-orbit interaction. $\tilde{\boldsymbol{J}}^z$ is the spin current vector carrying the z-component of the spin in the local spin basis.

Further, the dynamics of a domain wall in a Josephson junction under the action of torques (30)-(31) is analyzed analytically and numerically. The results obtained show that the dynamics of domain walls under the action of supercurrent can be fully implemented in modern Josephson junctions through strong ferromagnets. The results of this subsection were obtained in collaboration with A.M. Bobkov and M.A. Silaev and published in **[P20]** from the author's list of publications on the topic of the dissertation.

Section **4.2** predicts and discusses the chiral triple spin interaction carried by the condensate. This interaction breaks the symmetry with respect to the inversion of the magnetic moment. The proposed interaction mechanism removes the degeneracy between topologically different magnetic textures and enables low-dissipation manipulation of magnetic defects, such as skyrmions. The possibility of such an interaction can be understood from the symmetry arguments. Consider the simplest example of three magnetic moments $\boldsymbol{m}_{1,2,3}$ localized in a metal that does not contain other magnetic moments and in the absence of a magnetic field. An energy contribution proportional to the spin chirality $E_{ch} = E_a \boldsymbol{m}_1 \cdot (\boldsymbol{m}_2 \times \boldsymbol{m}_3)$ is only possible if the scalar prefactor E_a changes sign with time reversal $\mathcal{T}$. Since we assume that there are no other magnetic moments in the metal, such a scalar $E_a \neq 0$ cannot be constructed in the normal state. In the dissertation, this is shown using a direct calculation. However, odd relative $\mathcal{T}$ scalars exist in the superconducting state when the condensate

moves with a nonzero velocity $\boldsymbol{v}_s \neq 0$. This breaks the symmetry with respect to time reversal and one can choose as E_a the projection of the superfluid velocity onto some anisotropy axis determined, for example, by the spatial configuration of the magnetic moments. Therefore, in the superconducting state with $\boldsymbol{v}_s \neq 0$, chiral-selective triple spin interactions are, generally speaking, possible.

The mechanism discussed above may be important for various hybrid S/F systems, as well as for interacting magnetic impurities in superconductors and magnetic atoms placed on a superconducting surface. Such systems are currently being actively studied in connection with topological quantum computing and spintronic applications based on low dissipative control of magnetic textures.

As the simplest example of a chiral triple interaction, the disseration considers three magnetic impurities with moments $\boldsymbol{m}_{1,2,3}$ located at the points $\boldsymbol{r}_l = (x_l, 0, 0)$ with $x_1 = 0$, $x_2 = d$, $x_3 = 2d$ along the x axis. It is shown that as a result of the exchange interaction with conduction electrons with constant J in the presence of a moving condensate, an additional contribution to the energy arises in the system, which is proportional to the scalar spin chirality $\chi = \boldsymbol{m}_1 \cdot (\boldsymbol{m}_2 \times \boldsymbol{m}_3)$ and in the limit of small temperatures $T \ll \Delta$ and distances between impurities $\Delta d/v_F \ll 1$ has the form:

$$E_{ch}(d) = 3\chi p_F v_s \frac{\pi^2 (N_0 J)^3}{2X^3}, \tag{32}$$

where $X = p_F d$. Note that we have obtained a result that does not contain Friedel oscillations on the scales of the Fermi wavelength. This shows that the triple interaction is carried exclusively by Cooper pairs without the participation of single-particle excitations.

The interaction mechanism (32) is fundamentally different from exchange and DM interactions. It can manifest itself in various systems containing magnetic moments and moving condensate. An important class of such systems are Josephson junctions through textured ferromagnets. An analogue of the condensate velocity in such systems is the phase difference between the superconducting electrodes. Therefore, for a fixed phase difference, magnetic textures with opposite chiralities will have different Josephson energies. As an example, the dissertation considers left and right magnetic spirals

$$\boldsymbol{m}(x) = \pm \boldsymbol{x} \cos\alpha + \sin\alpha (\boldsymbol{y} \cos\theta + \boldsymbol{z} \sin\theta) \tag{33}$$

with $\theta(x) = qx$ and $\alpha = const$. In the case of a weak proximity effect, for example, due to the low transparency of the barrier at the S/F interface, the current-phase relationship contains only the first harmonic

$$j = j_o \sin\varphi + j_a \cos\varphi. \tag{34}$$

Here the first term is the usual sinusoidal contribution with amplitude j_o. The second, anomalous, term is proportional to the spin chirality $j_a \propto \chi$, which can be defined in various ways depending on the system under consideration.

In a number of earlier works that considered the Josephson effect through a non-coplanar texture, for example, through a magnetic helix, vortex and skyrmion in weak ferromagnets, which are described by the quasiclassical Usadel theory, no anomalous Josephson effect was found. The general reason for this is the presence of an artificial symmetry $j(\boldsymbol{m}) = j(-\boldsymbol{m})$, which appears in quasiclassical equations. Together with the symmetry with respect to time reversal $j(\boldsymbol{m}, \varphi) = -j(-\boldsymbol{m}, -\varphi)$ it leads to the symmetry of the Josephson current with respect to phase reversal $j(\varphi) = -j(-\varphi)$, which disables anomalous current. To get rid

of this symmetry, we make the assumption that there are spin-filtering barriers at the S/F interfaces, which are characterized by the polarization vector $\boldsymbol{P}$. Such barriers can arise naturally, or they can be introduced into the system additionally. In this case, the situation $j(\boldsymbol{m}, \boldsymbol{P}) \neq j(-\boldsymbol{m}, -\boldsymbol{P})$ is possible, which makes it possible to break the symmetry of the Josephson current $j(\varphi) \neq -j(-\varphi)$ and, therefore, implement the anomalous Josephson effect. At the same time, this makes it possible to expand the class of spin-textured non-coplanar materials in which the anomalous Josephson effect can be expected. The B20 family of banded cubic helimagnets, MnSi, (Fe,Co)Si, and FeGe, can be considered as candidates.

Consider a magnetic texture in the form of a spiral (33) as a weak link of a Josephson junction. The presence of spin-filtering barriers with polarizations $\boldsymbol{P}_l$ and $\boldsymbol{P}_r$ on left and right interfaces, respectively, is assumed. We show that the chiral spin interaction selects a certain chirality of the magnetic configuration, i.e. the first term in the equation (33). This is equivalent to changing the sign of θ or the direction of the magnetization twist, which is determined by the sign of the gradient $\theta' \equiv \nabla_x \theta$. The spiral texture is described by three orthogonal vectors: $\boldsymbol{m} = \boldsymbol{M}/M$, and also

$$\boldsymbol{n}_\theta = -\partial_\theta \boldsymbol{m} \tag{35}$$

$$\boldsymbol{n}_\alpha = -(\partial_x \boldsymbol{n}_\theta \cdot \partial_\alpha \boldsymbol{m}) \partial_\alpha \boldsymbol{m}. \tag{36}$$

Of these, in combination with the polarization $\boldsymbol{P}$ of the spin-filtering barrier, one can write three different spin chiralities

$$\chi_1 = \boldsymbol{P} \cdot (\boldsymbol{n}_\alpha \times \boldsymbol{n}_\theta) \tag{37}$$

$$\chi_2 = \boldsymbol{P} \cdot (\boldsymbol{m} \times \boldsymbol{n}_\theta) \tag{38}$$

$$\chi_3 = \boldsymbol{P} \cdot (\boldsymbol{m} \times \boldsymbol{n}_\alpha) \tag{39}$$

Note that χ_1 is qualitatively different from $\chi_{2,3}$. While $\chi_{2,3}$ require a misorientation between the local exchange field and the boundary polarization, $\chi_1 \neq 0$ even if $\boldsymbol{P} \parallel \boldsymbol{m}$ is at the interface. Therefore, $\chi_{2,3}$ are associated with the outer "surface" chirality of the structure, and $\chi_1 = (\boldsymbol{P}\boldsymbol{m})\chi_{in}$, where $\chi_{in} = \boldsymbol{m} \cdot (\boldsymbol{n}_\alpha \times \boldsymbol{n}_\theta)$ is the intrinsic chirality of the magnetic texture. Consequently, χ_1 is the quantity that determines the anomalous Josephson effect in the case when both the polarization of the spin-filtering barrier and the magnetic texture originate from the same exchange field.

As a result of the calculation given in the dissertation, the current-phase relation is obtained, which has the form of the equation (34), where the anomalous current j_a is given by the sum of three contributions $j_a = j_{ex} + j_{in} + j_{mix}$. These three contributions are determined by different chiralities

$$j_{in} \propto (\chi_{1l} + \chi_{1r}) \tag{40}$$

$$j_{ex} \propto (\boldsymbol{P}_l \boldsymbol{m}_l + \boldsymbol{P}_r \boldsymbol{m}_r) \frac{(\chi_{2l}\chi_{3r} - \chi_{3l}\chi_{2r})}{\theta' \cos\alpha} \tag{41}$$

$$j_{mix} \propto (\chi_{1l} + \chi_{1r}) \left[\chi_{2l}\chi_{2r} + \frac{\chi_{3l}\chi_{3r}}{\theta'^2 \cos^2\alpha} \right] \tag{42}$$

where χ_{il} and χ_{ir} are the chirality values (37)-(39) computed on the left and right S/F interfaces and $\boldsymbol{m}_l = \boldsymbol{m}(0)$, $\boldsymbol{m}_r = \boldsymbol{m}(d)$.

The considered examples demonstrate that the triple spin interaction lifts the degeneracy of magnetic textures with opposite chiralities. In the general case, such an interaction arises in non-coplanar magnetic textures. Therefore, it is completely different from the situation in thin magnetic films, where Neel domain walls with left or right rotation of the magnetization

in the plane, which is fixed by a combination of the magnetostatic and DM contributions to the energy, become energetically more favorable. Unlike the non-coplanar textures considered here, it is impossible to assign a chirality to flat textures, defined as the mixed product $\boldsymbol{m}_1 \cdot (\boldsymbol{m}_2 \times \boldsymbol{m}_3)$. Due to the absence of this chiral invariant, flat textures with left and right turn of the magnetization remain degenerate with respect to the global magnetization inversion. The results were obtained in collaboration with A.M. Bobkov, D.S. Rabinovich and M.A. Silaev and published in **[P21]** from the author's list of publications on the topic of the dissertation.

The possibility of maintaining non-dissipative electric currents is considered to be the defining property of the superconducting state. However, this concept was revised after the discovery of type II superconductors, which can be in a mixed state characterized by the presence of Abrikosov vortices induced by a magnetic field. In general, the mixed state is resistive, since in the absence of a pinning potential, superconducting vortices begin to move under the action of an applied current. In this state, the motion of vortices generates an electric field, which leads to finite resistance and ohmic losses. Section **4.3** predicts another fundamental mechanism that can bring a superconducting system into a resistive state, ideally for an arbitrarily small applied current. Namely, it is shown that in S/F hybrid systems the dynamics of magnetization, which is generated by supercurrent, necessarily induces an electric field and energy losses, to some extent similar to the motion of Abrikosov vortices in type II superconductors. However, there is no complete analogy between these fundamental effects. In the case of a hybrid S/F system, the generation of an electric field is caused by the dynamics of the magnetization and energy losses occur in the magnetic subsystem through the Gilbert damping mechanism.

The scheme of the system under consideration is shown in Fig. 22(a). Its magnetic part consists of a ferromagnetic strip and is conceptually close in configuration to a race-track memory based on domain walls. The position of the domain walls in the strip can be controlled using the normal current j_N, which is applied along the strip. In addition, the system has two superconducting electrodes that form a Josephson junction on the ferromagnetic strip. The Josephson current in such a geometry has already been measured through the halfmetallic ferromagnet CrO_2 [27] for distances between superconducting electrodes much larger than the typical size of domain walls of the order of 20 nm.

As discussed in the previous sections, in such a system a gauge vector potential appears in the local spin basis. The reason for its occurrence may be SOC or texture non-coplanarity. It induces an anomalous phase shift and, in the case where the magnetization is time dependent, it also generates an electromotive force [28–30]. This situation is the focus of this section. The electromotive force must be compensated by the voltage that is induced at the junction. This voltage just supports the motion of the domain wall, compensating for the energy dissipation due to Gilbert damping by the power of the current source, as shown in the dissertation.

In the considered S/F/S junction, the coupled dynamics of the magnetization $\boldsymbol{M}$ and the Josephson phase difference φ is defined by a system of equations:

$$j = j_c \sin\left(\varphi - \varphi_0\{\boldsymbol{M}\}\right) + \frac{\dot{\varphi} - \dot{\varphi}_0\{\boldsymbol{M}\}}{2eRS}. \tag{43}$$

$$\frac{\partial \boldsymbol{M}}{\partial t} = -\gamma \boldsymbol{M} \times \boldsymbol{H}_{eff} + \frac{\alpha}{M} \boldsymbol{M} \times \frac{\partial \boldsymbol{M}}{\partial t} + \boldsymbol{T}, \tag{44}$$

Eq. (43) is a nonequilibrium current-phase relation that generalizes the resistively shunted (RSJ) model. It is written in a gauge-invariant form, including the anomalous phase shift

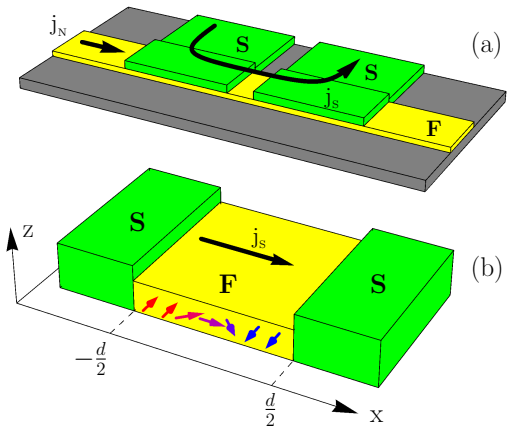

Figure 22: (a) Sketch of the system considered in section **4.3**. The superconducting electrodes that form the Josephson junction lie on a ferromagnetic strip. The position of the domain walls in the strip can be controlled by the normal current j_N. (b) Simplified model of the Josephson junction region. There is a Neel-type domain wall in the weak link region.

$\varphi_0\{\boldsymbol{M}\}$, which is determined by SOC and magnetic texture. For strong ferromagnets, only spin-triplet pairs with equal spins can penetrate F. Then the transport can be calculated in a local spin basis on split Fermi surfaces for spin up and down separately, with an effective U(1) spin-dependent gauge field $\boldsymbol{Z}$, which gives

$$\varphi_0\{\boldsymbol{M}\} = -2\int\limits_{-d/2}^{d/2} Z_x(x,t)dx. \tag{45}$$

where $\boldsymbol{Z} = \boldsymbol{Z}^m + \boldsymbol{Z}^{so}$. Here $Z_i^m = -i\mathrm{Tr}\left(\hat{\sigma}_z\hat{U}^\dagger\partial_i\hat{U}\right)/2$ is the contribution induced by the magnetic texture, where $\hat{U}(\boldsymbol{r},t)$ is a time-dependent and space-dependent unitary 2×2 matrix that rotates the spin quantization axis z to the local direction of the exchange field. The term $Z_j^{so} = (M_i B_{ij})/M$ comes from SOC.

Unlike the previous gauge non-invariant formulations [31, 32], Eq. (43) also takes into account normal magnetoelectric (spin-galvanic) effects at $j_c = 0$, such as the electromotive force and electric currents that are generated in a ferromagnet due to the time dependence of the Berry phase. A similar equation is also valid for the more general case of a non-sinusoidal dependence of the current-phase ratio.

Let us apply a constant Josephson current $I = jS$ (S is the junction area) to the Josephson junction and consider the stationary motion of the domain wall through the junction at a constant velocity. In this case, Eq. (43) can be easily solved and the time-averaged voltage that is induced on the junction is:

$$\overline{V(t)} = RS\sqrt{j^2 - j_c^2} + \frac{\pi\beta^2 u}{e\alpha d_W}, \tag{46}$$

where β is a dimensionless SOC constant. The first term is the well-known Josephson voltage, which appears at $j > j_c$. The second term V_M is nonzero both for $j > j_c$ and for $j < j_c$ and reflects the fact that the Josephson junction is always in a resistive state if the domain wall moves under the action of current. The corresponding IV characteristic of the

junction has a finite slope below the critical current. In principle, in point or small-area Josephson junctions with high resistance, the shunting capacitance or inductance can also lead to a finite slope of the IV-characteristic below the critical current. At the same time, the experimentally realized junctions through metallic ferromagnets practically do not show noticeable slopes of this branch. However, even if a finite slope due to interaction with the environment is present in the current-voltage characteristic, it can be easily distinguished experimentally from the effect discussed in this section by comparing the IV-characteristic of the junction in the presence of a domain wall and without it. Numerical estimates carried out in the dissertation give $V_M|_{j=j_c}$ up to $10^{-5} - 10^{-3}V$.

In practice, the motion of a domain wall can be induced by large current pulses. For short pulses, the domain wall does not leave the junction area during the pulse. In the dissertation, the dependences of the voltage on time for this case are calculated and it is shown that the presence of a moving wall leads to a strong change in this dependence. The results were obtained jointly with A.M. Bobkov, D.S. Rabinovich and M.A. Silaev and published in **[P22]** from the author's list of publications on the topic of the dissertation.

Section **4.4** is devoted to consideration of the direct and inverse magnetoelectric effects in thin-film bilayer superconductor/textured ferromagnet systems. A generalization of the quasiclassical theory is developed, which makes it possible to describe these effects. It is shown that the polarization of conduction electrons in a superconductor, which is induced as a result of the direct magnetoelectric effect, creates a torque that acts on the texture. The inverse magnetoelectric effect manifests itself in the form of phase-inhomogeneous superconducting states.

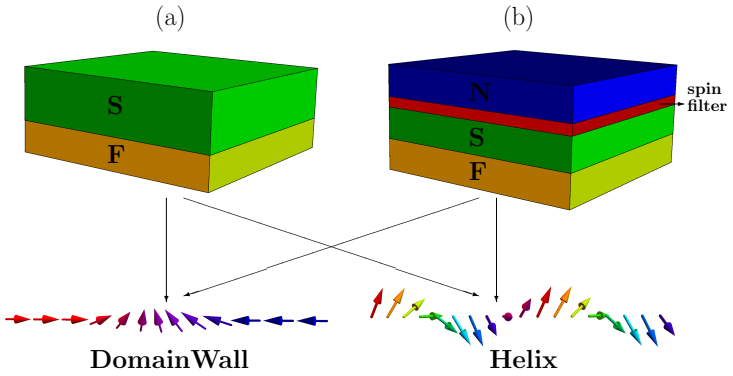

Figure 23: Sketches of the systems considered in section **4.4**. The left figure shows a possible implementation of an S/F bilayer consisting of a superconducting film and a strong ferromagnet. The right figure shows a possible implementation of an S/F bilayer with a weak ferromagnet and a spin-filtering layer. The spin-filtering interface and the weak ferromagnet are separated by a superconducting film so that the directions of their magnetizations can be independent of each other. The magnetic textures under consideration are shown at the bottom of the figure.

It is shown that the minimum necessary generalization of the Usadel equation, which allows one to describe magnetoelectric effects, is the inclusion of a spin-dependent depairing term, which modifies the diagonal potential in the Usadel equation

$$\check{\Lambda} = \check{\Lambda}_0 + i\Gamma \mathrm{sgn}\omega(\hat{\tau}_z + \boldsymbol{P}\hat{\boldsymbol{\sigma}}) \tag{47}$$

Then the effective 2D Usadel equation is as follows

$$-D\partial_{\boldsymbol{r}}\left(\check{g}\partial_{\boldsymbol{r}}\check{g}\right)+\left[(\omega+\mathrm{sgn}\omega\Gamma)\hat{\tau}_z-i\boldsymbol{h}_{eff}\hat{\boldsymbol{\sigma}}\hat{\tau}_z+\mathrm{sgn}\omega\Gamma\boldsymbol{P}\hat{\boldsymbol{\sigma}}+i\check{\Delta}(\boldsymbol{r}),\check{g}\right]=0, \tag{48}$$

where $\partial_{\boldsymbol{r}}=(\partial_x,\partial_y)$. Qualitatively, the last term in the equation (47) describes the suppression of superconductivity in the film due to the spin-dependent tunneling of electrons that make up Cooper pairs into a ferromagnet, and Γ is the effective depairing parameter. Polarization $\boldsymbol{P}$ describes the efficiency and quantization axis of the spin filter acting on electrons during tunneling between the superconductor and the adjacent layer, ferromagnetic or normal. It is this polarization $\boldsymbol{P}$ that makes it possible to break the symmetry $\boldsymbol{j}(\boldsymbol{M})=\boldsymbol{j}(-\boldsymbol{M})$, which is the reason for the absence of magnetoelectric effects in the quasiclassical approximation. The reason is that to obtain $\boldsymbol{P}\neq 0$, one must consider the exchange field of the spin-filtering layer (made of a strong ferromagnetic metal or ferromagnetic insulator) beyond the limits of the quasiclassical approximation, or, in other words, take into account the difference between the momenta of electrons with spins up and down within this layer.

On the basis of the equation (48) in the disseration, phase-inhomogeneous states are obtained in the systems shown in Fig. 23. In the case of a helical texture, a helical state with a constant phase gradient is realized in a superconductor. In the limit of slow spirals $\xi_S/L\ll 1$ and small values of Γ, the phase gradient has the form:

$$\partial_x\varphi_0=4\pi^2\chi_{int}P\sin^2\theta\frac{D\Gamma}{L^2}\left(\frac{\sum\limits_{\omega>0}f_z^2/(\omega+\Gamma)^2}{\sum\limits_{\omega>0}[f_0^2+f_z^2]}\right), \tag{49}$$

where f_0 and f_z are the values of the singlet and triplet (for pairs with opposite spins) anomalous Green's functions of the superconductor, $\chi_{int}=\hat{\boldsymbol{h}}(\boldsymbol{n}_\theta\times\boldsymbol{n}_\delta)$ is an invariant describing the internal chirality of the helix. It is assumed here that the polarization vector $\boldsymbol{P}$ is codirectional with the local magnetization of the magnet. $P\chi_{int}$ is the same chiral invariant that was introduced in section **4.2** to describe the anomalous Josephson effect in S/F/S junctions through a helical ferromagnet. This shows the universality of the chiral nature of the inverse magnetoelectric effect in superconducting hybrid systems with textured ferromagnets.

The dissertation also considers a phase-inhomogeneous state that occurs in the presence of a domain wall in a ferromagnet. In this case, a spontaneous phase difference appears in the superconductor in the vicinity of the wall, which, in the same approximations as for the spiral texture, has the form:

$$\Delta\varphi_0=2\pi\Gamma|P_\perp|\chi_{ex}\frac{\sum\limits_{\omega>0}f_z^2/(\omega+\Gamma)}{\sum\limits_{\omega>0}[f_0^2+f_z^2]}. \tag{50}$$

The dissertation considers the case of a flat domain wall. Therefore, it has no internal chirality and the magnetoelectric effect arises due to the external chirality $\chi_{ex}=\mathrm{sgn}\left[\boldsymbol{P}(\partial_x\hat{\boldsymbol{h}}\times\hat{\boldsymbol{h}})\right]$, $P_\perp$ component of the polarization vector $\boldsymbol{P}$ perpendicular to the plane of the domain wall. The outer chirality is nonzero when the polarization $\boldsymbol{P}$ of the spin-filtering interface has a component perpendicular to the wall plane. To study a wider range of system parameters, the dissertation also carried out numerical calculations of inhomogeneous phase states.

The phase difference arising in the superconductor due to the magnetoelectric effect provides a link between the magnetic texture and the condensate phase. In particular,

this provides a method for the electrical detection of time-dependent textures (for example, moving domain walls or other magnetic defects) through the relation $V = (\hbar/2e)\partial_t \Delta\varphi$. It is interesting that such detection makes it possible to determine not only the defect velocity, but also its chirality.

Let us now consider the direct magnetoelectric effect in S/F bilayers, i.e. generation of equilibrium spin polarization in response to supercurrent. The dissertation shows that the induced spin polarization has a component that is perpendicular to the magnetization of the ferromagnet and therefore creates a torque acting on the ferromagnetic texture $\boldsymbol{M}(\boldsymbol{r})$. For an arbitrary magnetic texture, under the condition that the spatial change in the magnetization is slow and the depairing parameter Γ is small, the torque has the form:

$$\boldsymbol{N} = b_j \partial_x \hat{\boldsymbol{h}} + c_j \chi_{int} (\tilde{\boldsymbol{P}}_\perp \times \hat{\boldsymbol{h}}), \tag{51}$$

$$c_j = \pi \mu_B N_F T D \partial_x \varphi \sum_{\omega>0} \frac{8\beta h \Gamma \Delta f_z}{(\omega+\Gamma)[(\omega+\Gamma)^2 + h_{eff}^2]}, \tag{52}$$

$$b_j = c_j (\boldsymbol{P}\hat{\boldsymbol{h}}), \tag{53}$$

Here χ_{int} is the local internal chirality of the magnetic texture, defined in the same way as for a magnetic spiral, and β is a dimensionless phenomenological coefficient, the value of which depends on a specific microscopic model describing the exchange interaction between the conduction electrons of a superconductor and the magnetization ferromagnet. The first term in the equation (51) is the adiabatic torque. Usually, the adiabatic torque is determined by the transfer of angular momentum from the current-carrying electrons to the magnetization of the ferromagnet. Therefore, the coefficient b_j is proportional not only to the electric current j, but also to the degree of spin polarization. In our case, the microscopic origin of the adiabatic torque is somewhat different. Let us first consider the case when $\boldsymbol{P}$ is codirectional with the magnetization of the ferromagnet. Then $\tilde{\boldsymbol{P}}_\perp = 0$ and the adiabatic torque is the only contribution to the torque acting on the magnetization of the ferromagnet. It can be shown that in this case the spin current flowing through the system vanishes with the accuracy considered. Therefore, the electric current is not spin-polarized and the torque is not related to the derivative of the spin current, i.e. with the transfer of the spin moment from the conduction electrons to the magnetization of the ferromagnet. The mechanism of the appearance of torque is due to the fact that the flowing supercurrent generates spin splitting of the density of states in the superconductor.

If $\boldsymbol{P}$ is not completely co-directed with the magnetization of the ferromagnet, then another part of the torque appears, which is expressed by the second term of the equation (51). In the general case, this contribution has components both along the $\partial_x \hat{\boldsymbol{h}}$ direction and along the $\hat{\boldsymbol{h}} \times \partial_x \hat{\boldsymbol{h}}$ direction perpendicular to it. But it cannot be included in either the adiabatic or non-adiabatic torque, because it is proportional to the intrinsic chirality of the χ_{int} structure and hence vanishes for coplanar magnetic textures. The results were obtained in collaboration with D.S. Rabinovich, A.M. Bobkov and M.A. Silaev and published in **[P23]** from the author's list of publications on the topic of the dissertation.

In the conclusions the main results of the work and its conclusions are formulated.

Conclusions

In the author's opinion, the results of the dissertation work indicate that the well-known properties of the superconducting state - absence of the dissipation, the macroscopic nature of the condensate phase and the gap in the density of states on the Fermi surface, in combination

with wide possibilities for designing various types of spin-orbit coupling and the coexistence of superconductivity and magnetism in heterostructures make it possible to realize and explore rich new physics. This, in turn, makes superconducting heterostructures a promising platform for low-dissipation spintronics.

References

[1] M. Eschrig, Spin-polarized supercurrents for spintronics: a review of current progress, Rep. Prog. Phys. **78** 104501 (2015).

[2] J. Linder and J.Robinson, Superconducting spintronics, Nature Physics **11** 307 (2015).

[3] V. V. Ryazanov, V. A. Oboznov, A. Yu. Rusanov, A. V. Veretennikov, A. A. Golubov, and J. Aarts, Coupling of Two Superconductors through a Ferromagnet: Evidence for a Junction. Phys. Rev. Lett. **86**, 2427 (2001).

[4] F. S. Bergeret, M. Silaev, P. Virtanen, and T. T. Heikkila, Colloquium: Nonequilibrium effects in superconductors with a spin-splitting field, Rev. Mod. Phys. **90**, 041001 (2018); T. T. Heikkila, M. Silaev, P. Virtanen, and F. S. Bergeret, Thermal, electric and spin transport in superconductor/ferromagnetic-insulator structures, Progress in Surface Science **94**, 100540 (2019).

[5] I. V. Bobkova, A. M. Bobkov, and M. A. Silaev, Magnetoelectric effects in Josephson junctions (Topical Review), J. Phys.: Condens. Matter **34**, 353001 (2022).

[6] Yu. M. Shukrinov, Anomalous Josephson effect, Phys.-Usp. **65**, 317 (2022).

[7] S. Mironov, A. S. Mel'nikov, and A. Buzdin, Electromagnetic proximity effect in planar superconductor-ferromagnet structures, Appl. Phys. Lett. **113**, 022601 (2018).

[8] G. A. Bobkov, I. V. Bobkova, A. M. Bobkov, Long-range interaction of magnetic moments in a coupled system of S/F/S Josephson junctions with anomalous ground state phase shift, Phys. Rev. B **105**, 024513 (2022).

[9] A.I. Larkin and Yu.N. Ovchinnikov, Nonuniform state of superconductors, Sov. Phys. JETP **20**, 762 (1965) [Zh. Eksp. Teor. Fiz. **47**, 1136 (1964)].

[10] P. Fulde and R.A. Ferrel, Superconductivity in a Strong Spin-Exchange Field, Phys.Rev. **135**, A550 (1964).

[11] A. I. Buzdin, Proximity effects in superconductor-ferromagnet heterostructures, Rev. Mod. Phys. **77**, 935 (2005).

[12] F. S. Bergeret, A. F. Volkov, K. B. Efetov, Odd triplet superconductivity and related phenomena in superconductor-ferromagnet structures, Rev. Mod. Phys. **77**, 1321 (2005).

[13] A. M. Clogston, Upper Limit for the Critical Field in Hard Superconductors, Phys. Rev. Lett. **9**, 266 (1962).

[14] J. Baselmans, A. Morpurgo, B. Van Wees, and T. Klapwijk, Reversing the direction of the supercurrent in a controllable Josephson junction, Nature **397**, 43 (1999).

[15] F. Hubler, M.J. Wolf, D. Beckmann, and H.v. Lohneysen, Long-Range Spin-Polarized Quasiparticle Transport in Mesoscopic Al Superconductors with a Zeeman Splitting, Phys. Rev. Lett. **109**, 207001 (2012).

[16] M.J. Wolf, F. Hubler, S. Kolenda, H.v. Lohneysen, and D. Beckmann, Spin injection from a normal metal into a mesoscopic superconductor, Phys. Rev. B **87**, 024517 (2013).

[17] M.J. Wolf, C. Surgers, G. Fisher, and D. Beckmann, Spin-polarized quasiparticle transport in exchange-split superconducting aluminum on europium sulfide, Phys. Rev. B **90**, 144509 (2014).

[18] C.H.L. Quay, D. Chevallier, C. Bena, M. Aprili, Spin imbalance and spin-charge separation in a mesoscopic superconductor, Nature Phys. 9, **84** (2013).

[19] S. U. Jen and L. Berger, Thermal domain drag effect in amorphous ferromagnetic materials. II. Experiments, J. Appl. Phys. **59**, 1285 (1986).

[20] W. Jiang, P. Upadhyaya, Y. Fan, J. Zhao, M. Wang, Li-Te Chang, M. Lang, K. L. Wong, M. Lewis, Y.-T. Lin, J. Tang, S. Cherepov, X. Zhou, Y. Tserkovnyak, R. N. Schwartz, and K. L. Wang, Direct Imaging of Thermally Driven Domain Wall Motion in Magnetic Insulators, Phys. Rev. Lett. **110**, 177202 (2013).

[21] F.S. Bergeret and I.V. Tokatly, Singlet-Triplet Conversion and the Long-Range Proximity Effect in Superconductor-Ferromagnet Structures with Generic Spin Dependent Fields, Phys. Rev. Lett. **110**, 117003 (2013).

[22] F.S. Bergeret and I.V. Tokatly, Spin-orbit coupling as a source of long-range triplet proximity effect in superconductor-ferromagnet hybrid structures, Phys. Rev. B **89**, 134517 (2014).

[23] V. M. Edelstein, Magnetoelectric effect in polar superconductors, Phys. Rev. Lett. **75**, 2004 (1995).

[24] A. Zyuzin, M. Alidoust, and D. Loss, Josephson junction through a disordered topological insulator with helical magnetization, Phys. Rev. B **93**, 214502 (2016).

[25] F. Sebastian Bergeret and Ilya V. Tokatly, Manifestation of extrinsic spin hall effect in superconducting structures: Nondissipative magnetoelectric effects, Phys. Rev. B **94**, 180502 (2016).

[26] M. B. Lifshits and M. I. Dyakonov, Swapping Spin Currents: Interchanging Spin and Flow Directions, Physical Review Letters **103**, 186601 (2009).

[27] A. Singh, C. Jansen, K. Lahabi, and J. Aarts, High-Quality CrO_2 Nanowires for Dissipationless Spintronics, Physical Review X **6**, 041012 (2016).

[28] K. W. Kim, J. H. Moon, K. J. Lee, and H. W. Lee, Prediction of Giant Spin Motive Force due to Rashba Spin-Orbit Coupling, Phys. Rev. Lett. **108**, 217202 (2012).

[29] G. Tatara, N. Nakabayashi, and K. J. Lee, Spin motive force induced by Rashba interaction in the strong s-d coupling regime, Phys. Rev. B **87**, 054403 (2013).

[30] Y. Yamane, J. Ieda, and S. Maekawa, Spinmotive force with static and uniform magnetization induced by a time-varying electric field, Phys. Rev. B **88**, 014430 (2013).

[31] Yu. M. Shukrinov, I. R. Rahmonov, K. Sengupta, and A. Buzdin, Magnetization reversal by superconducting current in φ_0 Josephson junctions, Appl. Phys. Lett. **110**, 182407 (2017).

[32] F. Konschelle, A. Buzdin, Magnetic Moment Manipulation by a Josephson Current, Phys. Rev. Lett. **102**, 017001 (2009).